

Machine Learning and the Yield Curve: Tree-Based Macroeconomic Regime Switching

Siyu Bie
City University of Hong Kong

Francis X. Diebold
University of Pennsylvania

Jingyu He
City University of Hong Kong

Junye Li
Fudan University

First Draft: July 2024
This Draft: August 26, 2024

Abstract: We explore tree-based macroeconomic regime-switching in the context of the dynamic Nelson-Siegel (DNS) yield-curve model. In particular, we customize the tree-growing algorithm to partition macroeconomic variables based on the DNS model's marginal likelihood, thereby identifying regime-shifting patterns in the yield curve. Compared to traditional Markov-switching models, our model offers clear economic interpretation via macroeconomic linkages and ensures computational simplicity. In an empirical application to U.S. Treasury bond yields, we find (1) important yield curve regime switching, and (2) evidence that macroeconomic variables have predictive power for the yield curve when the short rate is high, but not in other regimes, thereby refining the notion of yield curve “macro-spanning”.

Acknowledgments: We gratefully acknowledge helpful input from Sid Chib. All remaining errors are ours alone.

Keywords: Decision Tree; Macro-Finance; Term Structure; Regime Switching; Dynamic Nelson-Siegel Model; Bayesian Estimation

JEL Classification: C11, E43, G12

Contact Information: siyubie2-c@my.cityu.edu.hk (Bie); fdiebold@sas.upenn.edu (Diebold); jingyuhe@cityu.edu.hk (He); li_junye@fudan.edu.cn (Li)

1 Introduction

Yield curve modeling plays crucial roles in asset pricing, risk management, and monetary policy, and the Nelson-Siegel model (Nelson and Siegel, 1987) has long been popular among both researchers and practitioners for its parsimonious yield-curve representation. Diebold and Li (2006) propose a *dynamic* Nelson-Siegel (DNS) model, allowing for three unobserved pricing factors (level, slope, and curvature) that evolve smoothly.¹ In reality, however, the yield curve does not always move smoothly; its underlying factors can exhibit abrupt shifts or structural breaks, particularly in response to macroeconomic (e.g., business cycle) conditions. This highlights the importance of possible yield curve regime switching, and the importance of understanding how yield-curve regimes relate to macroeconomic conditions.

Economists have studied yield curve regime switching (e.g., Dai et al., 2007; Hevia et al., 2015), typically invoking Markov-switching behavior à la Hamilton (1989) and Kim (1994).² However, such models often lack clear economic interpretation, because their regimes are latent, which makes it difficult to understand what the “regimes” indicate. Although several studies interpret regimes in terms of macroeconomic conditions, such as real activity or asset market volatility (e.g., Hamilton, 1989; Bansal and Zhou, 2002), those interpretations have a strong flavor of Monday-morning quarterbacking. An economically interpretable methodology for detecting regime changes in the macroeconomy and relating them to the yield curve remains elusive and needs to be developed.

In this paper we fill the void by developing a novel DNS extension that incorporates regime switching, which we call *macro-instrumented DNS regimes*. We make two related contributions. First, we allow the DNS factors to switch dynamics across macroeconomic regimes, which we detect using a customized tree structure based on the values of an observable set of macroeconomic variables. Using Bayesian methods, we choose optimal split candidates based on the marginal DNS likelihood, which

¹See Diebold and Rudebusch (2013) for a full exposition with variations and extensions.

²See also Gray (1996), Ang and Bekaert (2002), Bansal and Zhou (2002), and Xiang and Zhu (2013).

enhances regime interpretability and provides a macroeconomically meaningful understanding of yield curve dynamics.³

Second, we address the long-standing issue of whether the yield curve spans the macroeconomy (“macro-spanning”), meaning that all current and past macroeconomic information is contained in the current yield curve. Such macro-spanning implies, among other things, that macroeconomic variables have no predictive content for the yield curve. The validity of macro-spanning, however, is far from uncontroversial. On the one hand, macro-spanning is a key implication of the hugely-popular class of affine macro-finance models, as reviewed for example in Bauer and Rudebusch (2017). In those models,

... the short-term interest rate is represented as an affine function of risk factors ... that include macroeconomic variables. Accordingly, the assumption of the absence of arbitrage and the usual form of the stochastic discount factor imply that model-implied yields are also affine in these risk factors. This linear mapping from macro factors to yields can ... be inverted to express the macro factors as a linear combination of yields. Hence, these models imply ... “spanning” ...,

(Bauer and Rudebusch, 2017)

and it has found some empirical support, as in Bauer and Rudebusch (2017). On the other hand, macro-spanning is rejected by several other studies, ranging from the early work of Ang and Piazzesi (2003) through more recent work like Joslin et al. (2014) and Bekaert et al. (2021).⁴ Those studies, however, are based on linear models, whereas we investigate macro-spanning through the more nuanced nonlinear lens of macro-instrumented regime switching, which allows for the possibility that macro-spanning might hold in some macroeconomic regimes but not in others.

We proceed as follows. In section 2 we review the DNS model and introduce our tree-based macro-instrumented regime-detection framework. In section 3 we present empirical results for U.S. treasury bonds. We conclude in section 4, and we provide supplementary derivations and empirical results in a series of appendices.

³Hence we make contact with two recent literatures – one that uses goal-orientated tree-based clustering with economic targets (e.g., Cong et al., 2022, 2023; Feng et al., 2024; Patton and Simsek, 2023), and one that implements Bayesian analysis of regression tree models (e.g., Chipman et al., 2010; He et al., 2019; He and Hahn, 2023; Krantsevich et al., 2023).

⁴See also Dewachter and Lyrío (2006), Diebold et al. (2006), Ludvigson and Ng (2009), Duffee (2011), Chernov and Mueller (2012), and Coroneo et al. (2016).

2 Dynamic Nelson-Siegel with Macro-Instrumented Regime Switching

In this section we introduce our modeling framework and estimation strategy, and we provide simulations documenting good performance.

2.1 The State-Space Model

We first review the dynamic Nelson-Siegel (DNS) model (Diebold and Li, 2006) and its extension to a macro-finance yield-curve model (Diebold, Rudebusch, and Aruoba, 2006). DNS extends the original static Nelson-Siegel model (Nelson and Siegel, 1987) by writing the time- t maturity- τ yield $y_t(\tau)$ as:

$$y_t(\tau) = L_t + S_t \left(\frac{1 - e^{-\lambda\tau}}{\lambda\tau} \right) + C_t \left(\frac{1 - e^{-\lambda\tau}}{\lambda\tau} - e^{-\lambda\tau} \right) + \varepsilon_t(\tau), \quad (1)$$

where λ controls the decay rate of the yield curve; the three parameters L_t, S_t, C_t are allowed to vary over time and are interpreted as level, slope, and curvature factors, respectively; $\varepsilon_t(\tau)$ is a stochastic shock capturing pricing error; and $t = 1, \dots, T$. The full measurement equation relating the N observed yields to the three latent factors is then

$$\begin{pmatrix} y_t(\tau_1) \\ y_t(\tau_2) \\ \dots \\ y_t(\tau_N) \end{pmatrix} = \begin{pmatrix} 1 & \frac{1-e^{-\lambda\tau_1}}{\lambda\tau_1} & \frac{1-e^{-\lambda\tau_1}}{\lambda\tau_1} - e^{-\lambda\tau_1} \\ 1 & \frac{1-e^{-\lambda\tau_2}}{\lambda\tau_2} & \frac{1-e^{-\lambda\tau_2}}{\lambda\tau_2} - e^{-\lambda\tau_2} \\ \dots & \dots & \dots \\ 1 & \frac{1-e^{-\lambda\tau_N}}{\lambda\tau_N} & \frac{1-e^{-\lambda\tau_N}}{\lambda\tau_N} - e^{-\lambda\tau_N} \end{pmatrix} \begin{pmatrix} L_t \\ S_t \\ C_t \end{pmatrix} + \begin{pmatrix} \varepsilon_t(\tau_1) \\ \varepsilon_t(\tau_2) \\ \dots \\ \varepsilon_t(\tau_N) \end{pmatrix}.$$

Finally, the DNS model assumes VAR(1) transition dynamics for the state vector $(L_t, S_t, C_t)'$, thus forming a well-defined state-space system.

We now allow for regime switching in the latent factors. Specifically, assume there are G regimes in total, and let $z_t = 1, 2, \dots, G$ indicate the regime label at time period t . We treat the number of regimes G and the regime labels z_t as exogenous for the moment, and we will discuss estimation (learning) subsequently. Conditional on all

regime labels, we can write the model as

$$\begin{aligned} \mathbf{y}_t &= \mathbf{\Lambda} \boldsymbol{\mu}_{z_t} + \mathbf{\Lambda} \mathbf{F}_t + \boldsymbol{\varepsilon}_t, \\ \mathbf{F}_t &= \mathbf{A}_{z_{t-1}} \mathbf{F}_{t-1} + \boldsymbol{\eta}_t, \end{aligned} \quad (2)$$

where $\mathbf{f}_t = (L_t, S_t, C_t)^T$ are the factors, $\mathbf{F}_t = \mathbf{f}_t - \boldsymbol{\mu}_{z_t}$ are the demeaned factors, and $\mathbf{y}_t = (y_t(\tau_1), \dots, y_t(\tau_N))^T$ are the N yields at the t -th period. In particular, we assume the transition equation may be affected by regime changes such that the mean of the factors, $\boldsymbol{\mu}_{z_{t-1}}$, and the VAR evolution matrix, $\mathbf{A}_{z_{t-1}}$, depend on the regime label, z_{t-1} , of the previous time period, which is determined conditional on the information set up to period $t - 1$ only. The mean vector, $\boldsymbol{\mu}_{z_{t-1}}$, and the evolution matrix, $\mathbf{A}_{z_{t-1}}$, correspond to all G regimes. Furthermore, we assume the measurement disturbances and the transition noises follow the standard assumptions of independence and joint normality,

$$\begin{pmatrix} \boldsymbol{\varepsilon}_t \\ \boldsymbol{\eta}_t \end{pmatrix} \sim \mathcal{N} \left(\mathbf{0}, \begin{pmatrix} \mathbf{Q} & \mathbf{0} \\ \mathbf{0} & \mathbf{H}_{z_t} \end{pmatrix} \right), \quad (3)$$

where the covariance of the factor innovation, \mathbf{H}_{z_t} , depends on the regime of the same period and is a dense matrix. We assume that the covariance of the measurement errors is diagonal, $\mathbf{Q} = \text{diag}(\sigma_1^2, \dots, \sigma_N^2)$, which means that the residuals of the yields at different maturities are uncorrelated.

The above model with three latent yield factors can be extended to a macro-finance version that allows exploration of the relationship between macroeconomic and yield factors. Following Diebold et al. (2006), we examine three major macroeconomic variables: manufacturing capacity utilization (CU_t), the federal funds rate (FFR_t), and annual price inflation ($INFL_t$). We set $\mathbf{m}_t = (CU_t, FFR_t, INFL_t)^T$, and augment the state-space model in Equation (2) with these three macroeconomic variables.

Let \mathbf{M}_t be the demeaned macroeconomic factors, $\mathbf{M}_t = \mathbf{m}_t - \boldsymbol{\mu}_{z_t}^m$, and $\mathbf{F}\mathbf{F}_t = (\mathbf{F}_t, \mathbf{M}_t)^T$, and assume that both the yield and macroeconomic factors $\mathbf{F}\mathbf{F}_t$ follow

VAR(1) processes. Then the augmented state-space model takes the form of

$$\begin{pmatrix} \mathbf{y}_t \\ \mathbf{m}_t \end{pmatrix} = \begin{pmatrix} \mathbf{\Lambda} & \mathbf{0} \\ \mathbf{0} & \mathbf{I}_3 \end{pmatrix} \mathbf{F}\mathbf{F}_t + \begin{pmatrix} \mathbf{\Lambda} & \mathbf{0} \\ \mathbf{0} & \mathbf{I}_3 \end{pmatrix} \boldsymbol{\mu}_{z_t} + \boldsymbol{\varepsilon}_t, \quad (4)$$

$$\mathbf{F}\mathbf{F}_t = \mathbf{A}_{z_{t-1}} \mathbf{F}\mathbf{F}_{t-1} + \boldsymbol{\eta}_t,$$

where $\mathbf{A}_{z_{t-1}} = \begin{pmatrix} \mathbf{A}_{z_{t-1}}^{FF} & \mathbf{A}_{z_{t-1}}^{FM} \\ \mathbf{A}_{z_{t-1}}^{MF} & \mathbf{A}_{z_{t-1}}^{MM} \end{pmatrix}$, $\boldsymbol{\mu}_{z_t} = (\boldsymbol{\mu}_{z_t}^F, \boldsymbol{\mu}_{z_t}^m)^T$, $\boldsymbol{\varepsilon}_t = (\boldsymbol{\varepsilon}_t^y, \boldsymbol{\varepsilon}_t^m)^T$, $\boldsymbol{\eta}_t = (\boldsymbol{\eta}_t^y, \boldsymbol{\eta}_t^m)^T$, and the measurement and transition shocks are assumed to have the same normal distribution as in Equation (3).

2.2 Bayesian Estimation

We proceed in two steps. First we assume exogenously-known regimes, and then we consider endogenous regime determination (learning).

2.2.1 Exogenously Known Regimes

We take a full Bayesian approach to estimate the parameters of the model using the Kalman filter/smoothing and Markov chain Monte Carlo (MCMC). The yields-only model and the yields-macro model will be used to represent models (2) and (4), respectively, throughout the paper. Yields-only signifies a model that is exclusively based on yields, and yields-macro refers to a model that incorporates both yields and macroeconomic variables. When the number of regimes is determined, say three, we also refer to the two models as the three-regime yields-only DNS model and the three-regime yields-macro DNS model, respectively.

Prior Specification. We use standard conjugate priors for all parameters. Nevertheless, here we highlight that we assume the Bayesian spike-and-slab prior (George and McCulloch, 1993) on the off-diagonal elements in \mathbf{A}_g for a regime g . Let $a_{j,k}^g$ denote the

(j, k) -th element of \mathbf{A}_g , in which case the prior is

$$\begin{aligned}\pi(a_{jj}^g) &\sim N(0, \xi_1^2), \quad \text{for diagonal elements} \\ \pi(a_{jk}^g \mid \gamma_{jk}^g) &\sim (1 - \gamma_{jk}^g)N(0, \xi_0^2) + \gamma_{jk}^g N(0, \xi_1^2), \quad \text{for } j \neq k \\ \gamma_{jk}^g &\sim \text{Bernoulli}(w),\end{aligned}$$

where we choose the hyperparameter w equal to 0.5, suggesting that we have agnostic beliefs about off-diagonal elements in \mathbf{A}_g .

The diagonal elements of \mathbf{A}_g capture the autocorrelations of the factors, for which we simply use the conjugate normal prior. In contrast, for off-diagonal elements we use the spike-and-slab prior, which is a popular prior for variable selection, as it shrinks weak signals towards zero while maintaining strong signals at values close to OLS estimates. Notice that in the yields-macro model, for each regime g , the matrix \mathbf{A}_g captures the dynamics of the latent yield and macroeconomic factors. Using the spike-and-slab prior on the off-diagonal elements helps with the sparse matrix estimation and investigating the macro-spanning issue under various macroeconomic regimes.

For the covariance matrices \mathbf{Q} and \mathbf{H}_g , we use the standard inverse Wishart prior. Because \mathbf{Q} is assumed to be diagonal, which suggests the yields with different maturities are independent, the inverse Wishart prior degenerates to the inverse Gamma prior for each diagonal element σ_i^2 . For the factor mean μ_g we use a Gaussian prior, and for the decay parameter λ we use a uniform prior. Thus we write

$$\begin{aligned}\mathbf{H}_g &\sim IW(\mathbf{m}_0, \mathbf{M}_0), \quad \boldsymbol{\mu}_g \sim \mathcal{N}(\underline{\boldsymbol{\mu}}, \underline{\mathbf{B}}), \\ \sigma_i^2 &\sim IG(\alpha, \beta), \quad \lambda \sim \text{Unif}(a, b).\end{aligned}$$

Finally, departing from Diebold and Li (2006) where λ is calibrated at a fixed constant (0.0609), we allow λ to be learned from the data and updated by a random-walk Metropolis-Hastings step. See Appendix A for details of all prior specifications and the Gibbs sampler for posterior inference.

Marginal Likelihood. We now discuss the marginal likelihood of the yields-macro model (4); the marginal likelihood of the yields-only model (2) is similar and is subsumed by the yields-macro model. Using the marginal likelihood is a standard Bayesian approach for model comparison and selection. The primary advantage is that the marginal likelihood integrates out unknown parameters *a priori*, making it solely a function of the data. This approach contrasts to the plug-in parameter estimation (such as MLE), which does not account for the estimation uncertainty and may lead to inaccurate model comparisons when the parameter estimates are noisy.

Let $\Theta = (\Lambda, \mathbf{F}_t, \{\mathbf{A}_g\}_{g=1}^G, \{\boldsymbol{\mu}_g\}_{g=1}^G, \{\mathbf{H}_g\}_{g=1}^G, \mathbf{Q})$ denote all parameters and latent factors in the model, and let $L(\mathbf{y}_t, \mathbf{m}_t, \mathbf{z}_t \mid \Theta)$ denote the likelihood of the model in Equation (4). The latent factors \mathbf{F}_t are unknown parameters that need to be estimated, and there can be as many as 1,800 for 600 months and three latent factors. By simply plugging in the MLE point estimates, the accumulated estimation error can be severe for the likelihood calculation. Thus, by first integrating out the latent factors \mathbf{F}_t , we obtain a partial marginal likelihood for one time period yield \mathbf{y}_t , macroeconomic variables \mathbf{m}_t , and indicator of regimes \mathbf{z}_t as follows:

$$\begin{aligned} L(\mathbf{y}_t, \mathbf{m}_t, \mathbf{z}_t \mid \Lambda, \{\mathbf{A}_g\}_{g=1}^G, \{\boldsymbol{\mu}_g\}_{g=1}^G, \{\mathbf{H}_g\}_{g=1}^G, \mathbf{Q}) &= \int L(\mathbf{y}_t, \mathbf{m}_t, \mathbf{z}_t \mid \Theta) d\mathbf{F}_t \\ &= \mathcal{N}(\Lambda \mathbf{F}_{t|t, \mathbf{F}_{t+1}} + \Lambda \boldsymbol{\mu}_{\mathbf{z}_t}, \Lambda \mathbf{P}_{t|t, \mathbf{F}_{t+1}} \Lambda^T + \mathbf{Q}), \end{aligned}$$

which is a normal density with detailed forms of the mean and covariance matrix provided in Appendix A. Furthermore, the full partial marginal likelihood for all periods $\mathbf{Y} = \{\mathbf{y}_t\}_{t=1}^T$, $\mathbf{M} = \{\mathbf{m}_t\}_{t=1}^T$ and $\mathbf{Z} = \{\mathbf{z}_t\}_{t=1}^T$ is

$$\begin{aligned} L(\mathbf{Y}, \mathbf{M}, \mathbf{Z} \mid \Lambda, \{\mathbf{A}_g\}_{g=1}^G, \{\boldsymbol{\mu}_g\}_{g=1}^G, \{\mathbf{H}_g\}_{g=1}^G, \mathbf{Q}) \\ = \prod_{t=1}^T L(\mathbf{y}_t, \mathbf{m}_t, \mathbf{z}_t \mid \Lambda, \{\mathbf{A}_g\}_{g=1}^G, \{\boldsymbol{\mu}_g\}_{g=1}^G, \{\mathbf{H}_g\}_{g=1}^G, \mathbf{Q}). \end{aligned} \quad (5)$$

Except latent factors \mathbf{F}_t , integrating all other parameters of Equation (5) further yields,

$$L(\mathbf{Y}, \mathbf{M}, \mathbf{Z}) = \int L(\mathbf{Y}, \mathbf{M}, \mathbf{Z} \mid \Lambda, \{\mathbf{A}_g\}_{g=1}^G, \{\boldsymbol{\mu}_g\}_{g=1}^G, \{\mathbf{H}_g\}_{g=1}^G, \mathbf{Q}) d\Lambda d\mathbf{A}_g d\boldsymbol{\mu}_g d\mathbf{H}_g d\mathbf{Q}, \quad (6)$$

which lacks a closed-form expression. To tackle this problem, we draw posterior samples using the Gibbs sampler and plug each pair of posterior draws into Equation (6) to evaluate the full marginal likelihood, and then we average across posterior samples. This effectively integrates parameters out numerically.

We now introduce our macro-instrumented regime-switching model, integrating it into the Bayesian estimation framework for the yields-macro model discussed above.

2.2.2 Endogenously Estimated Regimes (Learning)

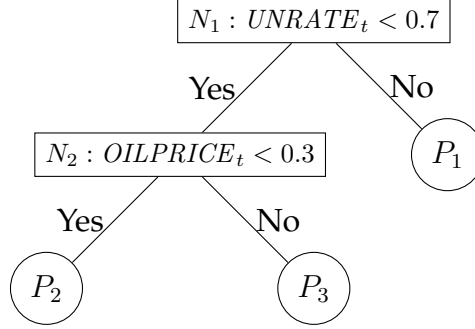
Thus far, the indicators of regimes $z_t \in \{1, 2, \dots, G\}$ and the total number of regimes G are assumed known. However, they should be learned from data jointly with all model parameters. In this section we present a model-based and macro-instrumented clustering approach to detect regimes. Our approach is model-based since the clusters are chosen according to valuations of the marginal likelihood of the model in Equation (4); it is macro-instrumented since all clusters are defined explicitly according to values of a set of macroeconomic variables.

The Classification and Regression Tree (CART) of Breiman et al. (1984) is one of the most successful machine learning non-parametric regression models for prediction. CART sequentially partitions data into multiple leaf nodes according to decision rules, which use one state variable at a time and compare it with a threshold. It then fits a constant to each leaf node for local prediction. Essentially, the CART fits a local constant step function to approximate any curve.

We borrow this divide-and-conquer strategy from CART. Similarly, we partition the data based on the value of macroeconomic variables to detect regimes. However, a significant distinction lies in our approach's focus on fitting the yields-macro model in Equation (4), where the choice of splitting values is determined by model fitness, specifically, the marginal likelihood of the model. Therefore, we interpret the decision tree more from the perspective of partitioning and identifying regimes rather than merely as a tool for generating step functions for prediction.

In Figure 1 we present a simple demonstration of decision tree structure consist-

Figure 1: An Illustrative Decision Tree



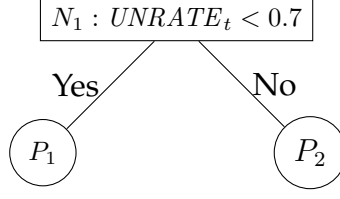
Notes: We illustrate a decision tree with two splits and three leaf nodes, creating three regimes based on macroeconomic variables, $UNRATE$ and $OILPRICE$, at thresholds of 0.7 and 0.3, respectively.

ing of two decision rules based on macroeconomic variables $UNRATE_t < 0.7$ and $OILPRICE_t < 0.3$, representing the unemployment rate and crude oil price at thresholds of 0.7 and 0.3, respectively. The top node N_1 is named the root node, which denotes all time periods. Two split points partition the root node into three regimes, denoted $\{P_1, P_2, P_3\}$. They are named as leaf nodes in the decision tree structure since they do not have any further splits. For instance, P_3 denotes regimes when the unemployment rate is less than 70% of the historical quantile and the oil price is higher than 30% of the historical quantile, and all the other regimes are interpreted similarly. For each time period t , starting from the top node of the decision tree, we compare the values of a set of macroeconomic variables at time t with all decision rules and eventually navigate to one and only one leaf node. The corresponding regime label z_t is simply the index of that leaf node.

Estimating the macro-instrumented regime-switching DNS model involves choosing the optimal splitting variables and thresholds from all candidates, along with estimating all parameters of the model in Equation (4). Specifically, when determining the optimal splitting variables, we evaluate the marginal likelihood, as discussed in the previous section, where all other model parameters are integrated out *a priori*.

Next, we illustrate the splitting algorithm step by step. Before the first split, the root node itself is a leaf node. This means that all time periods are homogeneous, and only one regime encompasses all periods, i.e., $z_t = 1$ for all $t = 1, \dots, T$. Then, we

Figure 2: Candidates of the First Decision-Tree Split



Notes: To determine the optimal split point, we evaluate many candidates (e.g., unemployment rate $UNRATE_t < 0.7$).

evaluate whether a split candidate is effective in partitioning the root, as illustrated in Figure 2. We need to define a measurement or split criterion to assess whether this split candidate can capture the regime pattern of the yield curve.

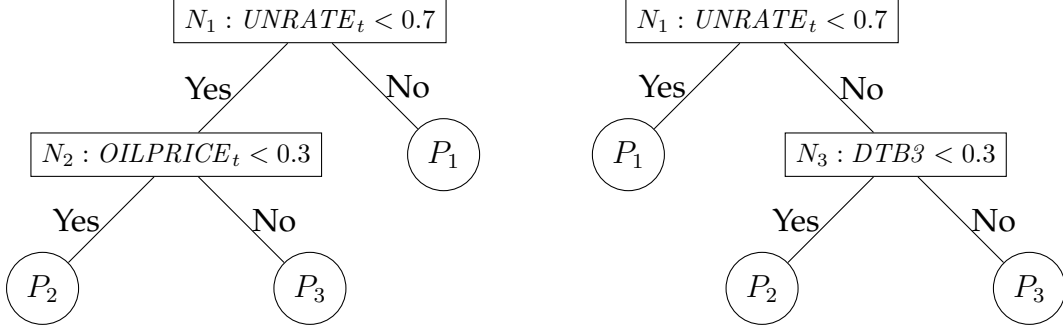
Suppose one split candidate based on unemployment rate $C_i : UNRATE_t < 0.7$ partitions the data to two disjoint potential regimes P_1 and P_2 , thus the regime indicators z_t are updated to reflect two regimes, $z_t^{C_i} = 1$ if $UNRATE_t < 0.7$ and $z_t^{C_i} = 2$ if $UNRATE_t \geq 0.7$. The new set of regime indicators are denoted as $\mathbf{Z}^{C_i} = \{z_t^{C_i}\}_{t=1}^T$ where the superscript emphasizes its dependence on specific split candidate C_i . The joint marginal likelihood is to evaluate Equation (6) with the new regime indicators,

$$L(C_i : UNRATE_t < 0.7) = L(\mathbf{Y}, \mathbf{M}, \mathbf{Z}^{C_i}). \quad (7)$$

We advocate using the marginal likelihood because it integrates unknown parameters *a priori*, accounting for parameter estimation uncertainty when determining regimes. While the yields \mathbf{Y} and the macroeconomic variables \mathbf{M} are fixed, the different split candidates create various regime partitions, yielding different regime indicators \mathbf{Z}^{C_i} and eventually leading to different evaluations of the split criterion in Equation (7). We loop over all potential split macroeconomic variables and thresholds and pick the one with the highest joint marginal likelihood as the first split point.

Once the first split is determined, the second split proceeds similarly. Figure 3 illustrates two potential ways to split since two leaf nodes are created after the first step. The second split can happen at either leaf node created by the first split, and

Figure 3: Candidates of the Second Decision-Tree Split



(a) Splitting node N_2 at $OILPRICE_t < 0.3$.

(b) Splitting node N_3 at $DTB3 < 0.3$.

Notes: The left and right panels (a) and (b) illustrate two potential candidates for the second split, where one of the nodes splits. Ultimately three leaf nodes (regimes) are available.

each has multiple potential macroeconomic variables and thresholds. Nevertheless, a candidate \mathcal{C}_i will create one more regime and end up with three. Let $\mathbf{Z}^{\mathcal{C}_i}$ denote the new regime indicators following the candidate tree structure with three regimes. Thus, the split criterion is defined as $L(\mathbf{Y}, \mathbf{M}, \mathbf{Z}^{\mathcal{C}_i})$ again, which varies with candidates since the indicators change while the yield and macro factors are fixed. We pick the one with the highest marginal likelihood.

All subsequent splits proceed similarly until some pre-specified stopping conditions are met. A tree can continue to grow with more splits, but a complex tree with many leaf nodes may suffer from poor generalizability and overfitting. Thus, the introduction of stopping rules is essential, such as the maximum depth, the maximum number of splits or leaf nodes, and the minimal number of observations in a leaf. If the tree reaches a pre-specified condition, the splitting process stops. In our setting, we restrict the number of regimes to be no more than 3, consistent with the existing literature (see, e.g., Xiang and Zhu, 2013). In addition, to ensure sufficient data for parameter estimation, we set the minimal number of months in a regime to 24 (2 years). Lastly, detecting regimes for the yields-only model proceeds similarly, with the only difference being using the yields-only model marginal likelihood as the split criterion.

Algorithm 1 summarizes the pseudocode for searching the macro-instrumented

Algorithm Macro-Instrumented Regime Clustering

- 1: Search all current leaf nodes $\mathcal{P} = \{P_1, \dots, P_J\}$.
- 2: **for** each leaf node $P_i \in \mathcal{P}$ **do**
- 3: **if** P_i satisfies minimal number of months in the node **then**
- 4: **for** each split variable and threshold combination $\mathcal{C}_{i,s} = \{x_i \leq c_s\}$ **do**.
- 5: Partition P_i to two leaf nodes P_i^{left} and P_i^{right} .
- 6: Update the regime indicators $\mathbf{Z}^{i,s}$ following the candidate structure
- 7: Calculate the split criterion in Equation (7) with new regime indicators

$$L_{i,s} = L(\mathbf{Y}, \mathbf{M}, \mathbf{Z}^{i,s})$$

- 8: **end for**
 - 9: **end if**
 - 10: **end for**
 - 11: Pick the optimal split point $C_{i,s}$ with largest marginal likelihood $L_{i,s}$, partition leaf node P_i according to $C_{i,s}$ and create two new leaf nodes.
 - 12: Check pre-specified stopping conditions such as maximum number of nodes, or depth. If satisfy then repeat from step 2, otherwise stop the algorithm.
-

regimes in the yields-macro model.

Once the splitting algorithm stops, the regime labels z_t for all time periods are determined explicitly by the tree structure, and we draw posterior samples of all parameters using the Gibbs sampler illustrated in Appendix A.

2.3 Simulation Evidence

We now explore the efficacy of our approach via a small simulation study. We generate the data following the three-regime yields-only model in Equation (2), where all underlying true parameters are calibrated using empirical data. We suppose that the true regimes are defined by two macroeconomic variables: inflation and unemployment rate, respectively, over the period from January 2001 to December 2022 (a total of 264 months), which are divided into three regimes: regime 1 with inflation less than 0.4, regime 2 with inflation greater than or equal to 0.4 and unemployment rate less than 0.2, and regime 3 with inflation greater than or equal to 0.4 and unemployment rate greater than or equal to 0.2. We use quantile values of the two variables in a rolling ten-year window in simulation.

In keeping with our empirical analysis in the next section, we assume that there are 13 yield maturities: 3, 6, 9, 12, 24, 36, 48, 60, 72, 84, 96, 108, and 120 months. We

Table 1: Simulation Results for Parameter Estimation, Three-Regime Yields Only Model

Panel A: Transition Matrix \mathbf{A} and Spike-and-Slab Prior Parameter γ									
	(1,1)	(2,1)	(3,1)	(1,2)	(2,2)	(3,2)	(1,3)	(2,3)	(3,3)
\mathbf{A}_1	0.99	0.00	0.00	0.00	0.98	0.00	0.05	0.10	0.92
$\widehat{\mathbf{A}}_1$	0.97	0.00	0.00	0.00	0.97	0.02	0.10	0.11	0.86
RMSE	0.02	0.00	0.00	0.00	0.02	0.02	0.05	0.01	0.06
MAE	0.02	0.00	0.00	0.00	0.01	0.02	0.05	0.01	0.06
$\widehat{\gamma}_1$	1.00	0.01	0.03	0.06	1.00	0.19	1.00	1.00	1.00
\mathbf{A}_2	0.98	0.00	0.00	-0.04	0.95	-0.20	0.00	0.00	0.90
$\widehat{\mathbf{A}}_2$	0.98	0.00	0.00	-0.03	0.93	-0.10	0.00	0.00	0.85
RMSE	0.00	0.00	0.00	0.01	0.02	0.10	0.00	0.00	0.05
MAE	0.00	0.00	0.00	0.01	0.02	0.10	0.00	0.00	0.05
$\widehat{\gamma}_2$	1.00	0.03	0.04	0.44	1.00	0.52	0.02	0.02	1.00
\mathbf{A}_3	0.97	0.00	0.00	-0.03	0.92	0.00	0.08	0.00	0.85
$\widehat{\mathbf{A}}_3$	0.98	0.00	0.00	0.00	0.87	0.00	0.07	0.00	0.93
RMSE	0.01	0.00	0.00	0.03	0.05	0.00	0.01	0.00	0.08
MAE	0.01	0.00	0.00	0.03	0.05	0.00	0.01	0.00	0.08
$\widehat{\gamma}_3$	1.00	0.02	0.05	0.03	1.00	0.07	1.00	0.02	1.00
Panel B: Factor Covariance Matrix \mathbf{H}									
	(1,1)	(2,1)	(3,1)	(1,2)	(2,2)	(3,2)	(1,3)	(2,3)	(3,3)
\mathbf{H}_1	0.07	-0.02	-0.03	-0.02	0.05	-0.07	-0.03	-0.07	0.50
$\widehat{\mathbf{H}}_1$	0.06	-0.01	-0.02	-0.01	0.05	-0.09	-0.02	-0.09	0.43
RMSE	0.01	0.01	0.01	0.01	0.00	0.02	0.01	0.02	0.07
MAE	0.01	0.01	0.01	0.01	0.00	0.02	0.01	0.02	0.07
\mathbf{H}_2	0.10	-0.08	-0.05	-0.08	0.12	0.04	-0.05	0.04	0.90
$\widehat{\mathbf{H}}_2$	0.10	-0.08	-0.08	-0.08	0.12	0.08	-0.08	0.08	0.83
RMSE	0.00	0.00	0.03	0.00	0.00	0.04	0.03	0.04	0.07
MAE	0.00	0.00	0.03	0.00	0.00	0.04	0.03	0.04	0.07
\mathbf{H}_3	0.18	-0.13	-0.20	-0.13	0.25	0.20	-0.20	0.20	1.18
$\widehat{\mathbf{H}}_3$	0.14	-0.12	-0.21	-0.12	0.25	0.29	-0.21	0.29	1.47
RMSE	0.04	0.01	0.01	0.01	0.00	0.09	0.01	0.09	0.29
MAE	0.04	0.01	0.01	0.01	0.00	0.09	0.01	0.09	0.29

Notes: In panel A we present results for transition matrix \mathbf{A} and spike-and-slab prior parameter γ , and in panel B we present results for the factor covariance matrix \mathbf{H} . We use three regimes and 13 yield maturities (3, 6, 9, 12, 24, 36, 48, 60, 72, 84, 96, 108, and 120 months). We simulate 100 sequences of monthly observations on yields with those maturities, and for each sequence we run our Bayesian estimation procedure and obtain posterior mean parameter estimates, tabulating the means and RMSEs (MAEs) of the posterior means across the 100 runs. (i, j) represents (i, j) -th element of a matrix. For the transition matrix, if \mathbf{A}_{ij} is not equal to 0, the corresponding value of γ is 1, otherwise 0.

Table 2: True and Estimated Values of Latent Factor Means

	L_t	S_t	C_t		L_t	S_t	C_t		L_t	S_t	C_t
μ_1	6.50	-1.80	-0.80	μ_2	6.00	-1.50	-0.50	μ_3	5.50	-1.20	-0.20
$\hat{\mu}_1$	7.46	-1.80	-1.05	$\hat{\mu}_2$	6.92	-1.71	-0.44	$\hat{\mu}_3$	6.39	-1.27	-0.21
RMSE	0.97	0.16	0.25	RMSE	0.93	0.26	0.11	RMSE	0.90	0.19	0.07
MAE	0.96	0.12	0.25	MAE	0.92	0.22	0.09	MAE	0.89	0.14	0.05

Notes: We show the true values (denoted μ) and estimated values (denoted $\hat{\mu}$) of the three latent factor means under three regimes, as well as MAE and RMSE measures of estimation accuracy.

Table 3: True and Estimated Value of Covariance Matrix \mathbf{Q}

	(1,1)	(2,2)	(3,3)	(4,4)	(5,5)	(6,6)	(7,7)	(8,8)	(9,9)	(10,10)	(11,11)	(12,12)	(13,13)
\mathbf{Q}	0.07	0.01	0.01	0.01	0.01	0.01	0.01	0.01	0.07	0.01	0.01	0.01	0.01
$\hat{\mathbf{Q}}$	0.07	0.01	0.01	0.01	0.01	0.01	0.01	0.01	0.08	0.01	0.01	0.01	0.01
RMSE	0.01	0.00	0.00	0.00	0.00	0.00	0.00	0.00	0.01	0.00	0.00	0.00	0.00
MAE	0.01	0.00	0.00	0.00	0.00	0.00	0.00	0.00	0.01	0.00	0.00	0.00	0.00

Notes: We show the true values (row \mathbf{Q}) and estimated values (row $\hat{\mathbf{Q}}$) of the 13 elements of the diagonal covariance matrix \mathbf{Q} , as well as MAE and RMSE measures of estimation accuracy. (i, j) represents (i, j) -th element of \mathbf{Q} .

generate 100 sequences of monthly observations on yields with those maturities and run estimation using our Bayesian method discussed above for each sequence of simulated data. In Table 1 we present simulation results for the transition matrix \mathbf{A} and the factor covariance matrix \mathbf{H} , and we report the results for other parameters in Tables 2 and 3. We report true values, means of posterior means, and RMSEs (MAEs) of posterior means across the 100 runs. We see that for almost all parameters, the means are very close to the true values, and the RMSEs (MAEs) are relatively small, suggesting that our approach provides accurate estimation of model parameters conditional on regimes.

3 Empirical Analysis of U.S. Treasury Bond Yields

Here we present an empirical study of U.S. Treasury bond yields. We examine two cases: one using only latent yield factors (the yields-only model, Equation (2)), and the other incorporating both latent yield factors and macroeconomic factors (the yields-macro model, Equation (4)). We evaluate the macro-instrumented regimes in both

Table 4: Descriptive Statistics for U.S. Yields

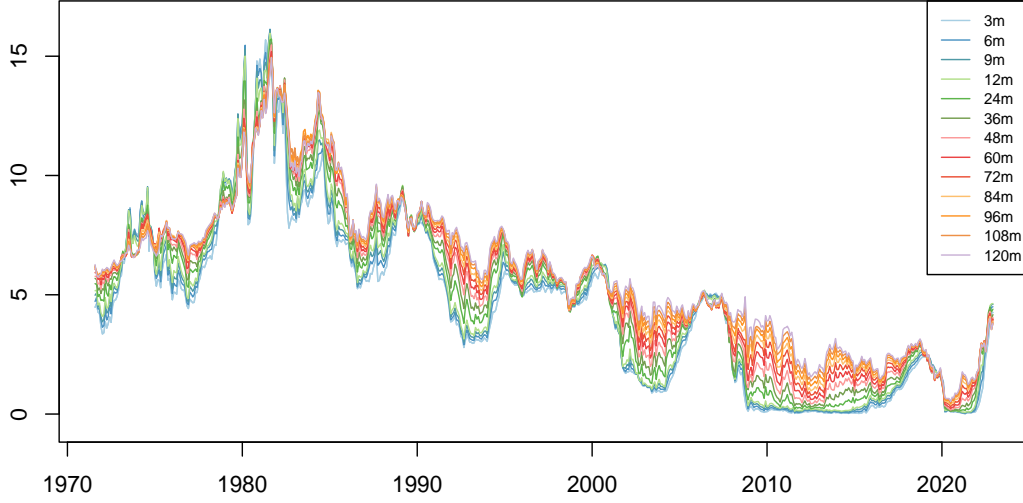
Maturity	Mean	Std	Min	Max	$\hat{\rho}(1)$	$\hat{\rho}(6)$	$\hat{\rho}(12)$	$\hat{\rho}(30)$
3	4.47	3.51	0.01	15.95	0.99	0.94	0.87	0.66
6	4.63	3.56	0.03	16.13	0.99	0.94	0.88	0.67
9	4.75	3.57	0.05	16.11	0.99	0.94	0.88	0.69
12	4.83	3.57	0.06	15.96	0.99	0.95	0.89	0.70
24	5.07	3.53	0.12	15.72	0.99	0.95	0.91	0.75
36	5.26	3.46	0.12	15.57	0.99	0.96	0.91	0.78
48	5.44	3.39	0.17	15.48	0.99	0.96	0.92	0.80
60	5.57	3.31	0.23	15.20	0.99	0.96	0.92	0.81
72	5.70	3.26	0.31	14.99	0.99	0.96	0.93	0.81
84	5.80	3.20	0.38	14.95	0.99	0.96	0.92	0.82
96	5.88	3.15	0.45	14.94	0.99	0.97	0.93	0.82
108	5.95	3.11	0.49	14.95	0.99	0.97	0.93	0.82
120	6.01	3.04	0.53	14.94	0.99	0.96	0.92	0.82

Notes: We present descriptive statistics for U.S. yields at various maturities, measured in months. The last four columns are sample autocorrelations at displacements of 1, 6, 12 and 30 months, respectively. The sample period is August 1971 - December 2022. The mean, standard deviation (Std), minimum (min) and maximum (max) values are expressed as percentages.

cases, focusing on the yields-macro model. Our primary interests are (1) determining whether regime switching exists, and if so, (2) understanding the interactions between macroeconomic factors and yield factors from the perspective of macro-spanning.

Most literature on yield curve regimes considers only two possible regimes and employs “Markov-switching” models, as for example in Dai et al. (2007) and Hevia et al. (2015). In contrast, we search for two sequential splits and create three macro-instrumented regimes with clear economic interpretations. The reasons for choosing three regimes are as follows. First, given the relatively small number of monthly data points, creating too many regimes may lead to fewer months in each regime and raise overfitting concerns. Second, our regimes are defined according to macroeconomic variables rather than time indexes, allowing a single regime to be projected over the time horizon with multiple disjoint intervals. Third, our approach chooses splits sequentially, with the importance of each split decreasing with its order. Thus, the first two splits that create three regimes are the most critical splits that identify macroeconomic regimes of the yield curve.

Figure 4: Time Series of U.S. Yields



Notes: We present time series of U.S. yields at maturities of 3, 6, 9, 12, 24, 36, 48, 60, 72, 84, 96, 108, and 120 months. The sample period is August 1971 - December 2022.

3.1 Data

We use the balanced zero-coupon U.S. Treasury bond yield data constructed by Liu and Wu (2021).⁵ The data are monthly, from August 1971 to December 2022, totaling 617 months, and they include 13 maturities of 3, 6, 9, 12, 24, 36, 48, 60, 72, 84, 96, 108, and 120 months for each time period. We show yield data descriptive statistics in Table 4 and time series in Figure 4. Among other things, it is apparent that (1) average yield increases with maturity, (2) yield volatility decreases with maturity, (3) long-maturity yields are more persistent than short-maturity yields, and (4) yield curves generally slope upward but are sometimes inverted.

As split candidates for detecting macroeconomic regimes, we use ten leading macroeconomic variables taken from the Federal Reserve Economic Data (FRED) database of the Federal Reserve Bank of St. Louis, listed in Table 5. In addition, we follow Diebold et al. (2006) in using three macroeconomic factors in our yields-macro model: manufacturing capacity utilization (CU_t), the federal funds rate (FFR_t), and annual inflation ($INFL_t$), along with three latent yield factors.

⁵Liu and Wu (2021) employ a kernel-smoothing method with adaptive bandwidth selection, which retains more of the information in the raw data, particularly for short and long maturities. The data are available at Cynthia Wu's website: <https://sites.google.com/view/jingcynthiawu/yield-data>

Table 5: Macroeconomic Variables Serving as Split Candidates

Variable	Description
$DTB3_t$	3-Month Treasury Bill Secondary Market Rate, Discount Basis
$INDPRO_t$	Industrial Production: Total Index (percent change from a year ago)
CPI_t	Consumer Price Index for All Urban Consumers (percent change from a year ago)
$M2_t$	Billions of Dollars, Seasonally Adjusted (percent change from a year ago)
$PAYEMS_t$	All Employees, Total Non-farm (percent change from a year ago)
$UNRATE_t$	Unemployment Rate
$OILPRICE_t$	Spot Oil Price: West Texas Intermediate (percent change from a year ago)
$TERM_SPREAD_t$	Term Spread
$DEFAULT_SPREAD_t$	Default Spread
VIX_t	CBOE Volatility Index

Notes: Data are from the Federal Reserve Economic Data (FRED) database maintained by the Federal reserve Bank of St. Louis.

We standardize the ten macroeconomic “split variables” on a rolling window basis. That is, instead of using raw values, we replace current macro values with quantiles in the past ten-year rolling-windows. Thus, all macroeconomic variable candidates are standardized within $[0, 1]$, and we use 0.2, 0.4, 0.6, and 0.8 as the candidate split thresholds for each variable.⁶ This standardization ensures that the splits are meaningful and comparable across different time periods.

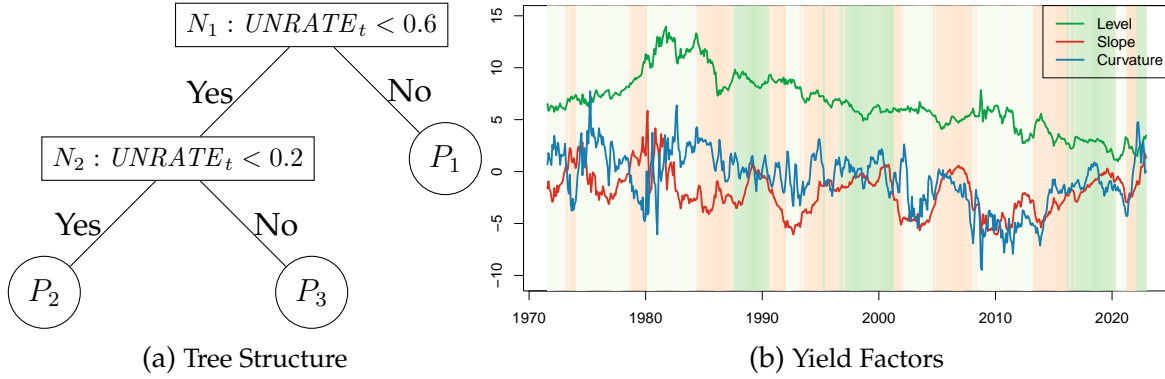
3.2 The Yields-Only Model

In Figures 5 and 6 we summarize and visualize the yields-only model estimation results. In the left panel of Figure 5 we detail the (three) estimated regimes. Both splits turn out to be driven by the unemployment rate. More specifically, the optimal splits are $UNRATE_t < 0.6$ and $UNRATE_t < 0.2$ at the first and second splits, respectively. Hence we divide our 617-month sample into the following three regimes: $UNRATE_t \geq 0.6$ (Regime 1, high-unemployment, 244 months), $UNRATE_t < 0.2$ (Regime 2, low unemployment, 150 months), and $0.2 \leq UNRATE_t < 0.6$ (Regime 3, medium unemployment, 223 months). In the right panel of Figure 5, we plot the extracted time series of latent level, slope and curvature yield factors, with regimes superimposed.

Next, in Figure 6 we show the actual and fitted yield curves, both overall and for

⁶Note that the three macroeconomic variables used in the yields-macro model for examining dynamic interactions with the yield factors are left unmodified with their original values.

Figure 5: Tree Structure and Time Series of Yield Factors, Three-Regime Yields-Only Model



Notes: In the left panel (a) we show the tree structure of estimated macro-instrumented regimes in the yields-only model. It partitions twice based on the unemployment rate, resulting in three regimes. In the right panel (b) we plot the three time series of latent yield factors extracted from the model, using background colors to indicate regime (light green for Regime 1, green for Regime 2, and orange for Regime 3).

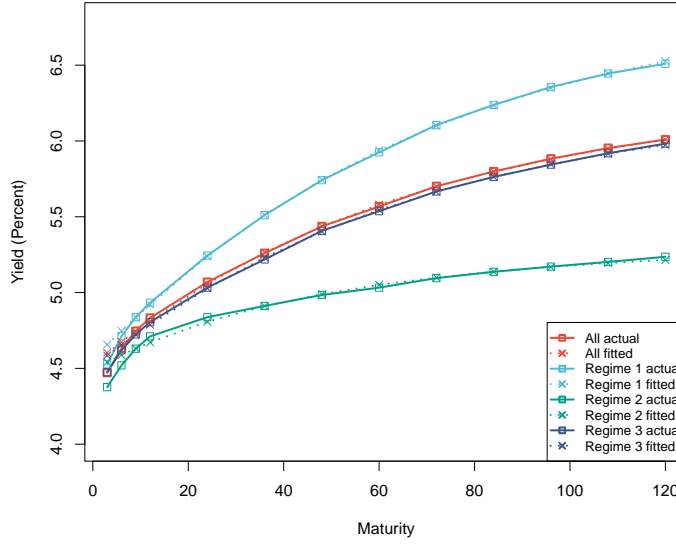
each of the three regimes.⁷ The model fits well, as the fitted curve is close to the actual one both overall and within each of the three regimes. Furthermore, we observe that yields are highest in Regime 1 when the unemployment rate is high (greater than the 60% quantile of the past ten years).

In Table 6 we present parameter estimation results. According to the estimated transition matrix A , the level factor is the most persistent and the curvature factor is the least persistent in all three regimes. We find that the curvature factor positively affects the future level factor in Regime 1 and positively affect the future slope factor in Regime 2. However, in Regime 3, we do not find any significant interactions among the three yield factors.

In Table 7 we present summary statistics of the yield residuals. Besides residual mean, standard deviation, minimum and maximum value, we also present mean absolute error (MAE) and root mean square error (RMSE) measuring the overall errors and model fitness. Broadly speaking, the three-regime yields-only DNS model fits the yield curve very well. On average, the MAE and RMSE are 4.69 bps and 6.61 bps, respectively. We note that the yields with 3- and 6-month maturities are relatively more challenging to fit and show higher pricing errors. In general, the model fits the long-

⁷We average the actual yield curves within the same regime.

Figure 6: Actual and Fitted Yield Curves, Three-Regime Yields-Only Model



Notes: We show actual yields and fitted yield curves in each of three estimated regimes, as well as over the full sample (“all actual” and “all fitted”).

maturity yields much better than the short-maturity yields. For example, the MAE for yields with maturities of 3-12 months is about 7.66 bps, whereas it is only 3.31 bps for yields with maturities of 60-120 months. This finding is consistent with the literature.

3.3 The Yields-Macro Model

We now present empirical results from the yields-macro regime-switching model in Equation (4). We find that when the macro factors are incorporated together with the yield factors, the split candidates change in comparison to those in the yields-only model, mainly because the joint dynamics of the macro and yield factors may exhibit different regime-switching patterns.

As we see from the left panel of Figure 7, the first split candidate is $DTB3_t$ (3-month treasury bill rate) at the threshold of 0.6, and the second is $UNRATE_t$ at the threshold of 0.4. The two splits create three regimes, Regime 1 ($DTB3_t \geq 0.6$) with 202 months, Regime 2 ($DTB3_t < 0.6$ & $UNRATE_t < 0.4$) with 169 months, and Regime 3 ($DTB3_t < 0.6$ & $UNRATE_t \geq 0.4$) with 246 months. In the right panel of Figure 7 we present the estimated time series of three yield factors. Despite the fact that the detected regimes are different, the factor dynamics look very similar to those resulting

Table 6: Parameter Estimates, Three-Regime Yields-Only Model

Regime 1	A			H			μ
	L_{t-1}	S_{t-1}	C_{t-1}	L_t	S_t	C_t	
L_t	0.98 (0.01)	0.00 (0.01)	0.03 (0.01)	0.21 (0.02)	-0.10 (0.02)	-0.35 (0.05)	6.18 (0.14)
S_t	0.00 (0.00)	0.96 (0.02)	0.00 (0.01)		0.55 (0.05)	0.10 (0.07)	-1.73 (0.12)
C_t	0.07 (0.05)	0.08 (0.05)	0.86 (0.04)			1.75 (0.17)	-0.78 (0.32)
Regime 2							
L_t	0.99 (0.01)	0.00 (0.00)	0.00 (0.00)	0.06 (0.01)	-0.03 (0.01)	0.03 (0.02)	6.11 (0.09)
S_t	0.00 (0.00)	0.95 (0.02)	0.09 (0.02)		0.10 (0.01)	-0.02 (0.02)	-1.39 (0.07)
C_t	0.00 (0.01)	0.00 (0.02)	0.83 (0.04)			0.46 (0.06)	-0.52 (0.19)
Regime 3							
L_t	0.99 (0.01)	0.01 (0.01)	0.00 (0.01)	0.10 (0.01)	-0.08 (0.01)	-0.06 (0.02)	6.13 (0.10)
S_t	0.00 (0.00)	0.99 (0.01)	0.00 (0.01)		0.22 (0.02)	0.11 (0.03)	-1.46 (0.10)
C_t	0.00 (0.01)	-0.02 (0.04)	0.92 (0.03)			0.76 (0.08)	-0.37 (0.27)

Notes: We show posterior means and standard deviations in each of the three regimes. Bold font indicates that the posterior 95% credible interval does not include 0. Because **H** is a symmetric matrix, we show only its diagonal and upper-right elements.

Table 7: Residuals, Three-Regime Yields-Only Model

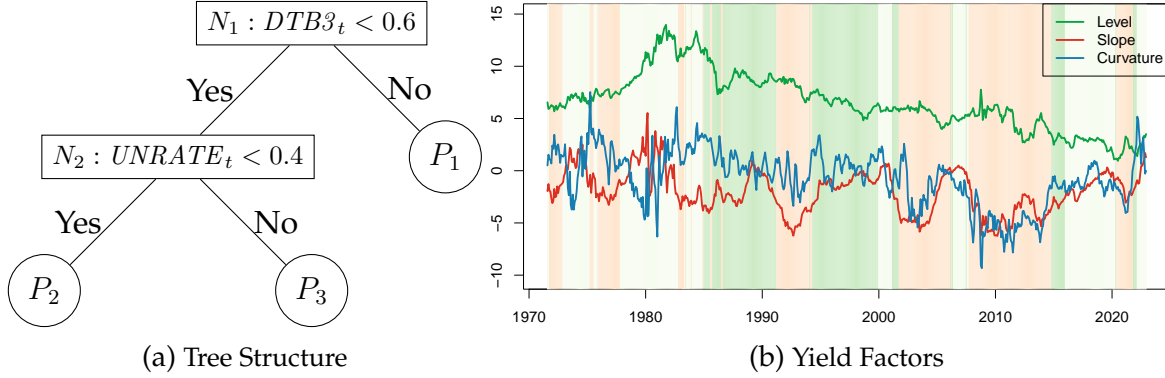
	Mean	Std	Min	Max	MAE	RMSE
3	-13.08	22.50	-129.55	51.24	18.76	26.01
6	-4.31	8.77	-51.63	28.73	7.30	9.76
9	0.13	0.83	-2.79	4.54	0.60	0.84
12	2.06	4.77	-24.10	24.23	3.99	5.19
24	1.15	7.32	-34.06	34.85	5.60	7.41
36	-0.48	4.09	-14.80	19.81	3.07	4.11
48	-0.05	2.45	-15.52	10.37	1.73	2.45
60	-1.26	4.42	-31.34	13.41	3.14	4.59
72	0.20	5.02	-17.42	25.33	3.48	5.02
84	0.03	3.90	-15.43	21.43	2.54	3.90
96	0.22	2.74	-14.80	17.07	1.59	2.75
108	0.30	4.93	-19.88	33.48	3.20	4.93
120	0.10	8.99	-49.67	19.90	5.94	8.98
3-12m	-3.80	9.21	-52.02	27.18	7.66	10.45
24-48m	0.21	4.62	-21.46	21.67	3.46	4.66
60-120m	-0.07	5.00	-24.76	21.77	3.31	5.03
Average	-1.15	6.21	-32.38	23.42	4.69	6.61

Notes: We show moments, extremes, MAE, and RMSE. Entries are in basis points.

from the yields-only model in the right panel of Figure 5.

In Table 8 we present the posterior means and standard deviations of the model parameters for the three regimes. Importantly, our results suggest that macro-spanning is regime-specific. In Regimes 2 and 3, we do not find any statistically significant effects of macro factors on yield factors (see estimates in the transition matrix **A**), suggesting that the macro factors have no predictive value for the yield curve. That is,

Figure 7: Tree Structure and Time Series of Yield Factors, Three-Regime Yields-Macro Model



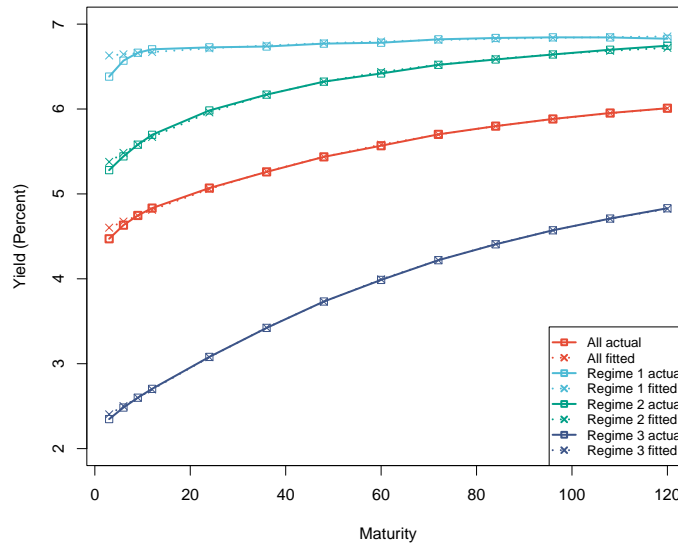
Notes: In the left panel (a) we show the tree structure of estimated macro-instrumented regimes in the yields-macro model. It partitions twice, based first on the 3-month interest rate and then on the unemployment rate, resulting in three regimes. In the right panel (b) we plot the three time series of latent yield factors extracted from the model, using background colors to indicate regime (light green for Regime 1, green for Regime 2, and orange for Regime 3).

macro spanning seems to be a reasonable approximation to the yields-macro dynamics in Regimes 2 and 3. In contrast, however, in Regime 1, which features high short-term (3-month) interest rates, we find a significant positive effect of inflation on the curvature factor, so that macro spanning is violated.

To further examine the macro-spanning issue, we estimate a yields-macro model with no regime switching, i.e., a single-regime model. We show the estimation results in Table 10. The effects of the macro factors on the yield factors are all statistically insignificant, providing further support to our finding that macro-spanning may be regime-specific and would be missed if one fails to allow for the possibility of regime switching.

In Table 9 we present summary statistics for the three-regime yields-macro model residuals. Overall, the model fits the yields well. In general it performs similarly to the yields-only model; for example, on average, the MAE and RMSE are 4.67 bps and 6.60 bps, respectively, which are the same as the corresponding values in the yields-only model. We also note that the yields-macro model performs slightly better than the yields-only model in fitting the short-maturity yields; for instance, the RMSEs for the 3- and 6-month yields are 25.88 bps and 9.68 bps, respectively, with comparison to

Figure 8: Actual and Fitted Yield Curves, Three-Regime Yields-Macro Model



Notes: We show actual yields and fitted yield curves in each of three estimated regimes, as well as over the full sample (“all actual” and “all fitted”).

26.01 bps and 9.76 bps, respectively, in the yields-only model.

Finally, it is interesting and informative to compare the fitted yield curves under the regimes identified by the yields-only model in Figure 6 to those resulting from the regimes identified by the yields-macro model which we show in Figure 8. Notably, the short-maturity yields are quite different in the three regimes in the yields-macro model, whereas they are similar in the three regimes in the yields-only model. This highlights that macro factors can help distinguish the regime-switching pattern in yield curves relative to using yield factors alone.

3.4 Comparing Regimes

Let us now explore further whether the three detected regimes are really different. To answer this question, we focus on the dynamics of factors, which are determined by the transition matrix A and factor innovation covariance matrix H . Therefore, we examine the difference between those two matrices under different regimes from both Bayesian and frequentist perspectives. We first overlay posterior distributions of the parameters and then conduct t -tests of the posterior samples across regimes.

Table 8: Parameter Estimates, Three-Regime Yields-Macro Model

Regime 1							H						μ
	L_{t-1}	S_{t-1}	C_{t-1}	CU_{t-1}	FFR_{t-1}	$INFL_{t-1}$	L_t	S_t	C_t	CU_t	FFR_t	$INFL_t$	
L_t	0.99 (0.01)	0.01 (0.02)	0.00 (0.00)	0.00 (0.00)	0.00 (0.01)	0.00 (0.00)	0.14 (0.02)	0.00 (0.02)	-0.21 (0.04)	0.05 (0.03)	0.07 (0.02)	0.01 (0.01)	5.83 (0.08)
S_t	0.00 (0.00)	0.92 (0.03)	0.00 (0.00)	0.00 (0.00)	0.00 (0.00)	0.00 (0.01)		0.61 (0.06)	-0.13 (0.07)	0.13 (0.06)	0.31 (0.05)	0.03 (0.02)	-1.25 (0.07)
C_t	0.00 (0.02)	-0.30 (0.07)	0.79 (0.04)	0.00 (0.00)	0.00 (0.02)	0.14 (0.03)			1.44 (0.16)	-0.01 (0.10)	-0.29 (0.07)	-0.03 (0.03)	0.11 (0.27)
CU_t	0.18 (0.18)	0.13 (0.16)	0.00 (0.01)	0.97 (0.02)	-0.16 (0.16)	-0.01 (0.02)				1.23 (0.14)	0.20 (0.06)	0.07 (0.02)	77.91 (0.18)
FFR_t	0.48 (0.05)	0.56 (0.05)	0.00 (0.00)	0.00 (0.00)	0.57 (0.04)	0.00 (0.00)					0.54 (0.06)	0.03 (0.02)	4.66 (0.07)
$INFL_t$	0.00 (0.00)	0.00 (0.00)	0.00 (0.00)	0.04 (0.00)	0.00 (0.00)	0.98 (0.01)						0.08 (0.01)	3.32 (0.06)
Regime 2													
L_t	0.98 (0.01)	0.00 (0.00)	0.00 (0.00)	0.00 (0.01)	0.00 (0.01)	0.00 (0.00)	0.09 (0.10)	-0.06 (0.06)	0.02 (0.03)	0.00 (0.01)	0.00 (0.09)	0.02 (0.02)	5.85 (0.11)
S_t	0.00 (0.00)	0.97 (0.02)	0.00 (0.01)	0.00 (0.01)	0.00 (0.02)	0.00 (0.00)		0.13 (0.05)	0.01 (0.02)	0.03 (0.02)	0.02 (0.06)	0.00 (0.01)	-1.38 (0.10)
C_t	0.00 (0.01)	0.00 (0.01)	0.88 (0.04)	0.00 (0.00)	0.00 (0.01)	0.00 (0.01)			0.48 (0.06)	0.04 (0.03)	0.00 (0.02)	0.01 (0.01)	-0.04 (0.24)
CU_t	0.00 (0.01)	0.00 (0.01)	0.00 (0.01)	0.98 (0.01)	0.00 (0.01)	0.00 (0.01)				0.28 (0.03)	0.02 (0.01)	0.03 (0.01)	77.87 (0.14)
FFR_t	0.34 (0.06)	0.30 (0.05)	0.00 (0.00)	0.00 (0.01)	0.68 (0.05)	0.00 (0.00)					0.05 (0.08)	0.01 (0.01)	4.71 (0.06)
$INFL_t$	0.00 (0.00)	0.00 (0.00)	0.00 (0.01)	0.00 (0.00)	0.00 (0.00)	0.99 (0.01)						0.05 (0.01)	3.28 (0.08)
Regime 3													
L_t	0.97 (0.01)	0.00 (0.00)	0.02 (0.01)	0.00 (0.02)	0.00 (0.02)	0.00 (0.00)	0.17 (0.48)	-0.13 (0.26)	-0.21 (0.13)	-0.01 (0.02)	-0.02 (0.42)	0.01 (0.07)	5.93 (0.12)
S_t	0.00 (0.01)	0.98 (0.01)	0.00 (0.02)	0.00 (0.01)	0.00 (0.03)	0.00 (0.01)		0.23 (0.17)	0.19 (0.07)	0.02 (0.02)	0.02 (0.22)	0.00 (0.03)	-1.43 (0.07)
C_t	0.00 (0.02)	0.00 (0.02)	0.93 (0.04)	0.00 (0.01)	0.02 (0.04)	0.00 (0.01)			1.10 (0.13)	0.02 (0.05)	0.02 (0.12)	0.02 (0.04)	-0.07 (0.34)
CU_t	-0.01 (0.03)	-0.02 (0.04)	0.07 (0.05)	0.98 (0.01)	-0.05 (0.05)	0.00 (0.01)				0.47 (0.05)	0.01 (0.01)	0.05 (0.01)	78.12 (0.13)
FFR_t	0.32 (0.05)	0.30 (0.04)	0.03 (0.01)	0.00 (0.02)	0.67 (0.04)	0.00 (0.00)					0.05 (0.36)	0.01 (0.06)	4.65 (0.06)
$INFL_t$	0.00 (0.01)	0.00 (0.01)	0.00 (0.01)	0.00 (0.00)	0.00 (0.01)	0.98 (0.01)						0.10 (0.02)	3.33 (0.06)

Notes: We show posterior means and standard deviations in each of the three regimes. Bold font indicates that the posterior 95% credible interval does not include 0. Because \mathbf{H} is a symmetric matrix, we show only its diagonal and upper-right elements.

Table 9: Residuals, Three-Regime Yields-Macro Model

	Mean	Std	Min	Max	MAE	RMSE
3	-13.04	22.37	-128.48	49.54	18.62	25.88
6	-4.29	8.69	-50.87	27.72	7.24	9.68
9	0.15	0.84	-2.28	3.78	0.62	0.85
12	2.06	4.77	-24.39	24.47	4.00	5.20
24	1.13	7.23	-33.52	34.17	5.51	7.31
48	-0.06	2.59	-16.90	11.20	1.80	2.59
84	0.03	3.90	-15.49	21.23	2.53	3.89
120	0.10	8.99	-50.30	21.09	5.95	8.98
3-12m	-3.78	9.17	-51.51	26.38	7.62	10.40
24-48m	0.19	4.60	-21.95	22.14	3.43	4.64
60-120m	-0.07	5.02	-25.06	22.01	3.33	5.05
Average	-1.15	6.20	-32.48	23.38	4.67	6.60

Notes: We show moments, extremes, MAE, and RMSE. Entries are in basis points.

Table 10: Parameter Estimates, Single-Regime Yields-Macro Model

	A						H						μ
	L_{t-1}	S_{t-1}	C_{t-1}	CU_{t-1}	FFR_{t-1}	$INFL_{t-1}$	L_t	S_t	C_t	CU_t	FFR_t	$INFL_t$	
L_t	0.98 (0.01)	0.00 (0.01)	0.01 (0.01)	0.00 (0.02)	0.01 (0.03)	0.00 (0.00)	0.15 (0.39)	-0.05 (0.06)	-0.14 (0.02)	0.01 (0.02)	0.00 (0.37)	0.01 (0.01)	6.36 (0.07)
S_t	0.00 (0.01)	0.96 (0.01)	0.01 (0.01)	0.01 (0.02)	0.00 (0.03)	0.00 (0.00)		0.34 (0.33)	0.05 (0.03)	0.05 (0.03)	0.09 (0.33)	0.01 (0.01)	-1.97 (0.05)
C_t	0.00 (0.02)	0.00 (0.02)	0.92 (0.02)	0.00 (0.00)	0.01 (0.02)	0.01 (0.02)			1.03 (0.07)	0.03 (0.04)	-0.10 (0.03)	0.00 (0.01)	-0.83 (0.25)
CU_t	0.30 (0.07)	0.23 (0.06)	0.02 (0.02)	0.99 (0.01)	-0.27 (0.06)	0.00 (0.01)				0.63 (0.04)	0.07 (0.02)	0.06 (0.01)	78.55 (0.14)
FFR_t	0.44 (0.04)	0.44 (0.04)	0.00 (0.01)	0.00 (0.02)	0.60 (0.03)	0.00 (0.00)					0.22 (0.35)	0.02 (0.01)	4.73 (0.05)
$INFL_t$	0.00 (0.00)	0.00 (0.00)	0.01 (0.01)	0.01 (0.00)	0.00 (0.00)	0.99 (0.00)						0.08 (0.00)	3.63 (0.06)

Notes: This table summarizes the posterior mean of parameter estimations. Bold font indicates that the posterior 95% credible interval does not cover 0. For simplicity, we only provide the diagonal and upper-right elements of \mathbf{H} given that \mathbf{H} is a symmetric matrix.

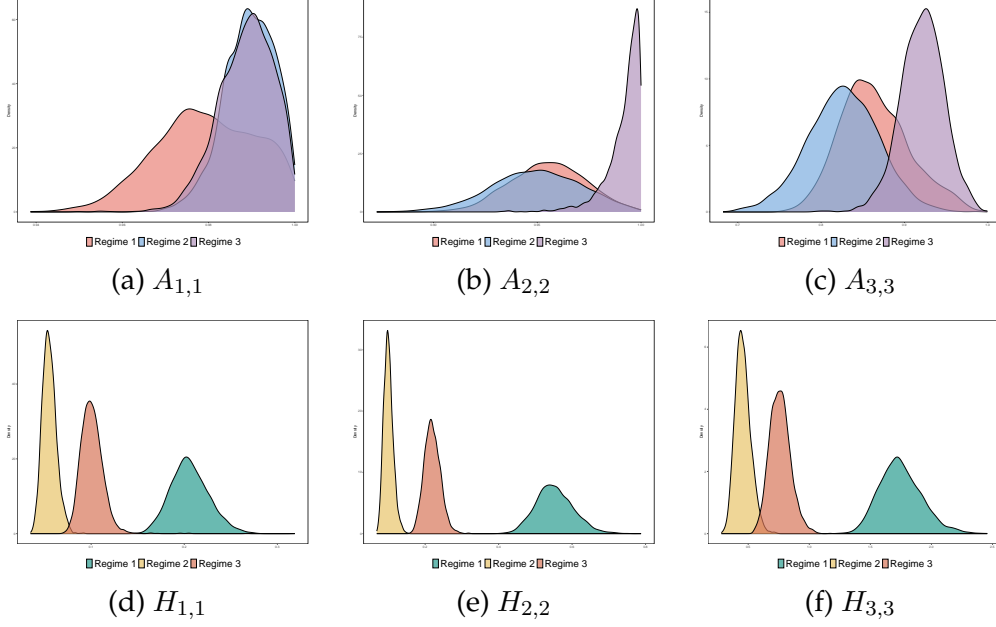
3.4.1 Posterior Distributions

We first examine more closely the posterior densities of the estimated parameters in \mathbf{A} and \mathbf{H} across different regimes. Given their importance in determining the factor dynamics, we focus on the diagonal elements, denoted by $A_{i,i}$ and $H_{i,i}$ for the i -th element on the diagonal respectively.

In Figure 9 we present posterior density plots for the yields-only model. It is clear that the three regimes detected are quite different for all pairs of regimes. For example, although Regimes 2 and 3 may have similar posterior densities for $A_{1,1}$, which represents the dynamics of the level factor, they are very different for $A_{2,2}$ and $A_{3,3}$ (slope and curvature factors, respectively). Notably, the factor innovation covariances are very different across regimes. The posterior densities of the diagonal elements of \mathbf{H} display only minimal overlap across the three regimes, which indicates that the factor dynamics change significantly under the three detected regimes.

In Figure 10 we present the corresponding posterior density plots for the yields-macro model. In parallel to the results for yields-only model, all parameters show very different posterior patterns across the identified regimes.

Figure 9: Posterior Densities of \mathbf{A} and \mathbf{H} , Three-Regime Yields-Only Model



Notes: We show posterior densities of the diagonal elements of the factor transition matrix \mathbf{A} and covariance matrix \mathbf{H} for the yields-only model with three regimes. Different colors indicate different regimes.

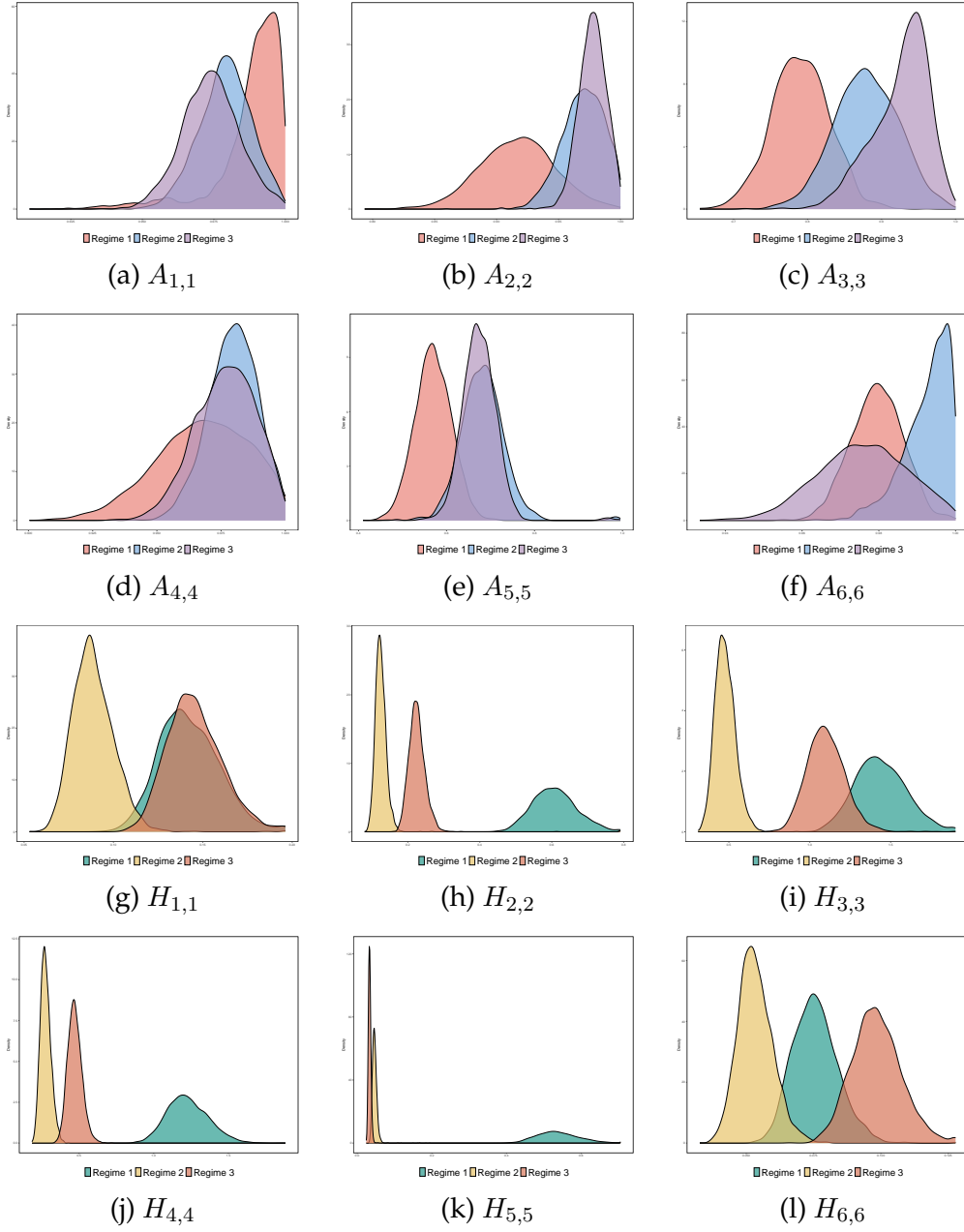
3.4.2 A Two-Sample t -Test

Here we further examine the differences among detected regimes using a simple t -test of the posterior samples of \mathbf{A} and \mathbf{H} . We focus on their diagonal elements for a concise presentation. The sample size is equal since we set equal posterior sample sizes n_s when estimating parameters in the Gibbs sampler. Given that we cannot ascertain identical variances among the regimes, we adopt the t -test that accounts for unequal variances of s_1^2 and s_2^2 . Our t -test statistic and its degrees of freedom are

$$t = \frac{\bar{X}_1 - \bar{X}_2}{s_\Delta}, \quad s_\Delta = \sqrt{\frac{s_1^2 + s_2^2}{n_s}}, \quad d.f. = \frac{(n_s - 1)(s_1^2 + s_2^2)^2}{s_1^4 + s_2^4}.$$

We show the test results of for yields-only and the yields-macro three regime DNS models in Table 11. It is clear that the three regimes identified in both models are significantly different.

Figure 10: Posterior Densities of \mathbf{A} and \mathbf{H} , Three-Regime Yields-Macro Model



Notes: We show posterior densities of the diagonal elements of the factor transition matrix \mathbf{A} and covariance matrix \mathbf{H} for the yields-macro model with three regimes. Different colors indicate different regimes.

3.5 Impulse Responses

Impulse response functions (IRFs) have been used at least since Sims (1980) to quantify the dynamic effects of shocks.⁸ Our focus is on differences in impulse re-

⁸We use generalized impulse response functions (Koop et al., 1996) because they are invariant to variable ordering.

Table 11: *t*-tests, Three-Regime Yields-Only and Yields-Macro Models

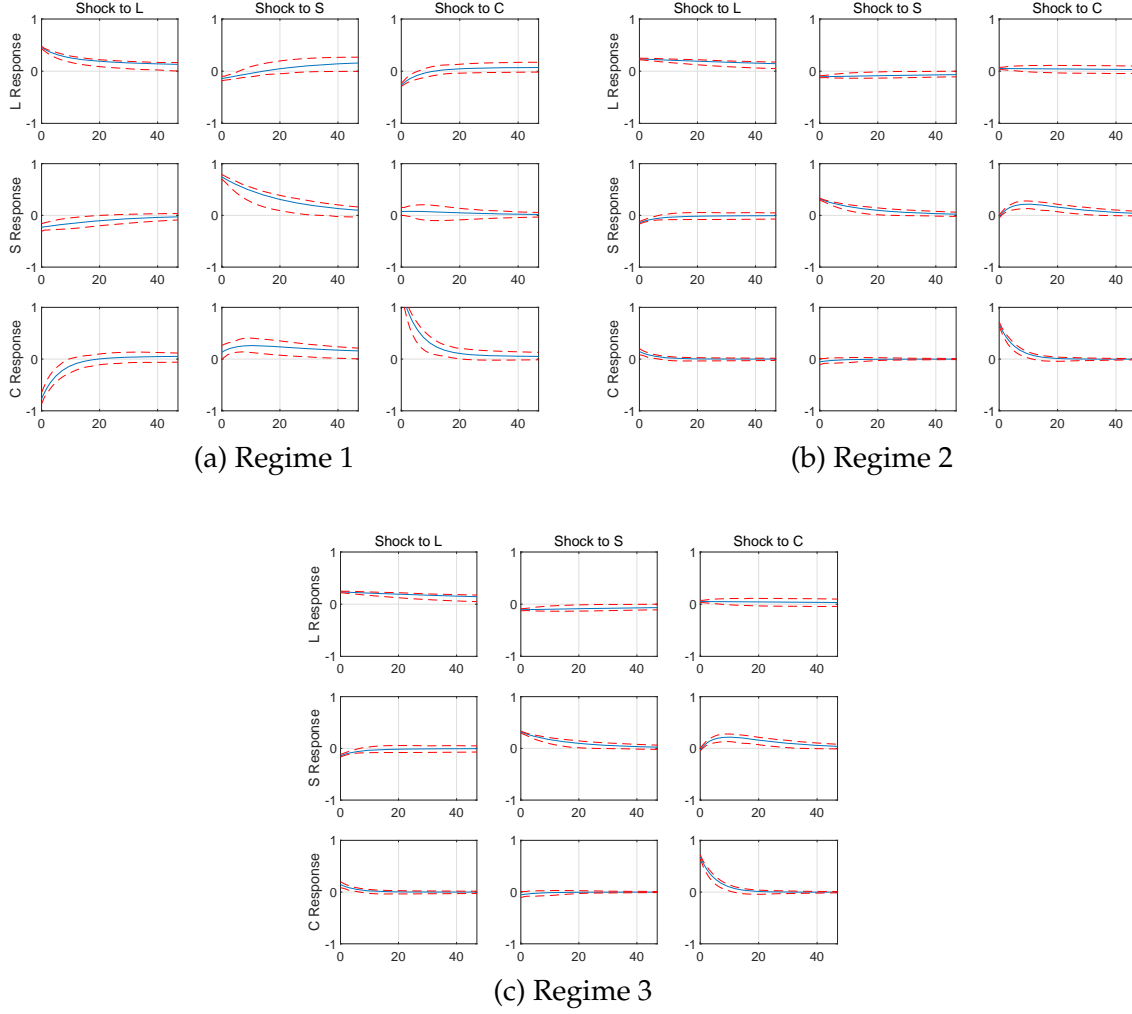
Models	Regimes	A			H		
			<i>t</i> -statistic	<i>p</i> -value		<i>t</i> -statistic	<i>p</i> -value
Yields-Only	1 vs 2	$A_{1,1}$	-42.61	0.00	$H_{1,1}$	378.51	0.00
		$A_{2,2}$	10.77	0.00	$H_{2,2}$	470.94	0.00
		$A_{3,3}$	34.79	0.00	$H_{3,3}$	384.73	0.00
	1 vs 3	$A_{1,1}$	-38.38	0.00	$H_{1,1}$	240.93	0.00
		$A_{2,2}$	-100.95	0.00	$H_{2,2}$	328.54	0.00
		$A_{3,3}$	-63.84	0.00	$H_{3,3}$	281.21	0.00
	2 vs 3	$A_{1,1}$	5.24	0.00	$H_{1,1}$	-174.01	0.00
		$A_{2,2}$	-100.46	0.00	$H_{2,2}$	-259.40	0.00
		$A_{3,3}$	-103.68	0.00	$H_{3,3}$	-157.14	0.00
Yields-Macro	1 vs 2	$A_{1,1}$	32.50	0.00	$H_{1,1}$	28.35	0.00
		$A_{2,2}$	-84.09	0.00	$H_{2,2}$	336.61	0.00
		$A_{3,3}$	-82.97	0.00	$H_{3,3}$	309.13	0.00
	1 vs 3	$A_{1,1}$	49.44	0.00	$H_{1,1}$	-2.58	0.01
		$A_{2,2}$	-102.33	0.00	$H_{2,2}$	117.09	0.00
		$A_{3,3}$	-135.42	0.00	$H_{3,3}$	89.82	0.00
	2 vs 3	$A_{1,1}$	20.47	0.00	$H_{1,1}$	-8.30	0.00
		$A_{2,2}$	-20.08	0.00	$H_{2,2}$	-33.33	0.00
		$A_{3,3}$	-44.13	0.00	$H_{3,3}$	-235.24	0.00
	1 vs 2	$A_{4,4}$	-32.08	0.00	$H_{4,4}$	368.43	0.00
		$A_{5,5}$	-93.53	0.00	$H_{5,5}$	272.98	0.00
		$A_{6,6}$	-79.05	0.00	$H_{6,6}$	112.93	0.00
	1 vs 3	$A_{4,4}$	-23.02	0.00	$H_{4,4}$	285.35	0.00
		$A_{5,5}$	-97.66	0.00	$H_{5,5}$	72.66	0.00
		$A_{6,6}$	15.37	0.00	$H_{6,6}$	-59.05	0.00
	2 vs 3	$A_{4,4}$	10.55	0.00	$H_{4,4}$	-183.32	0.00
		$A_{5,5}$	6.53	0.00	$H_{5,5}$	0.04	0.97
		$A_{6,6}$	70.62	0.00	$H_{6,6}$	-117.62	0.00

Notes: We show *t*-tests for the number of regimes in the yields-only and yields-macro models.

sponses across the three regimes. First, in Figure 11 we show IRFs and 90% confidence bounds for the yields-only model. The IRFs reveal significant differences across regimes; for example, given a shock to the level factor, the curvature factor decreases in Regime 1 but shows no obvious responses in Regimes 2 and 3.

Second, and of greater interest in terms of contributing to the macro-spanning debate, in Figure 12 we show Regime-1 IRFs and confidence bounds for the yields-macro model, and we group the IRFs into three panels: responses of yield factors to yield factors, responses of yield factors to macroeconomic factors, and responses of

Figure 11: Impulse Responses, Three-Regime Yields-Only Model



Notes: We show the full set of impulse response functions for each of the three regimes. Point estimates are blue and credible bands are red.

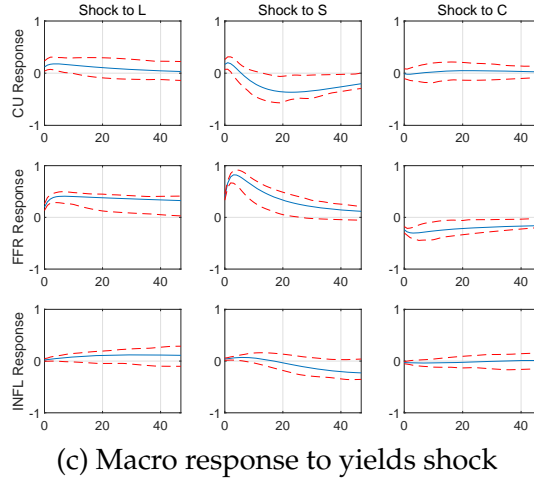
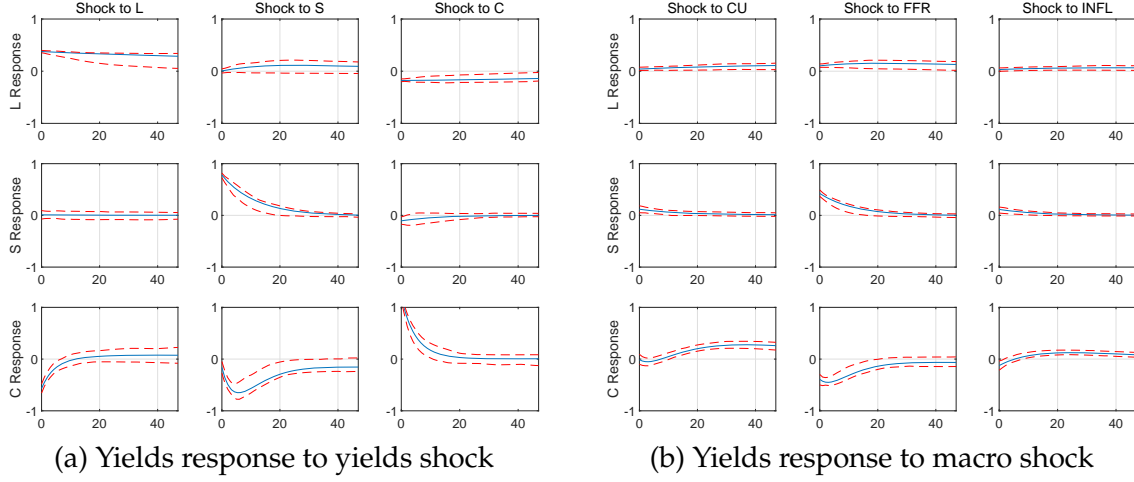
macroeconomic factors to yield factors.⁹

The Regime-1 level factor shows a positive but weak response to FFR_t shocks, and the slope factor shows a stronger positive response to FFR_t shocks. The curvature factor, moreover, appears to respond to shocks from all macro factors. This Regime-1 evidence against macro-spanning (i.e., evidence that macro \rightarrow yields) echoes the earlier-discussed yields-macro model parameter estimation results.

It should be noted however, that even if there is some macro \rightarrow yields predictive enhancement, it is not as strong or pervasive as the yields \rightarrow macro predictive enhancement. For example, FFR_t increases in response to shocks to the level and slope

⁹Results for Regimes 2 and 3 appear in Appendix B.

Figure 12: Impulse Responses in Regime 1, Three-Regime Yields-Macro Model



Notes: We show impulse responses for Regime 1. Point estimates are blue and credible bands are red.

factors in Regime 1. CU_t decreases in response to the slope factor in Regimes 1 and 3 and increases in response to the curvature factor in Regime 3. Additionally, $INFL_t$ decreases in response to an increase in the slope factor in Regime 1.

4 Conclusion

We explore tree-based macroeconomic regime-switching in the context of the dynamic Nelson-Siegel (DNS) yield-curve model. By integrating decision trees from machine learning, our approach customizes the tree-growing algorithm to partition macroeconomic variables based on the DNS model's Bayesian marginal likelihood, enabling us to identify regime-shifting patterns in the yield curve. Compared to tra-

ditional Markov-switching models, this “macro instrumented” approach offers clear economic interpretation via macroeconomic linkages and ensures computational simplicity.

We then provide a detailed empirical analysis of U.S. Treasury bond yields, August 1971 - December 2022. There are several findings. First, the macro-instrumented approach clearly identifies regime-switching behavior in both the yields-only and yields-macro models, both of which fit the data well. Second, the regimes are primarily driven by the unemployment rate in the yields-only model, whereas regimes are driven by the 3-month interest rate, followed by the unemployment rate, in the yields-macro model. Third, we find that in a regime with high 3-month interest rate (our “Regime 1”), the macro inflation factor contains useful information on the future yield curve, whereas in other regimes, macro factors do not contain any information on the future yield curve.

Overall, then, our results indicate not only that yields help forecast macro, but also that macro helps forecast yields, at least in a high-short-rate regime. That is, they suggest that macro spanning may fail in some regimes and hold in others. Professional thinking therefore needs some re-orientation – the right question is not “Does macro spanning hold or fail?”, but rather, “*When* does macro spanning hold, and *when* does it fail?”. We hope that our macro-instrumented regime-switching DNS model will continue to be a useful tool for navigating this new, more nuanced, environment.

Appendices

A Details of Posterior Inference

This section introduces the details of the Gibbs sampler for posterior inference. First we clarify notations: let $\tilde{\mathbf{y}}_T = [\mathbf{y}_1, \dots, \mathbf{y}_T]^T$, $\tilde{\mathbf{F}}_T = [\mathbf{F}_1, \dots, \mathbf{F}_T]^T$ be the collection of all data observations and latent factors. Let $\boldsymbol{\Omega} = [\mathbf{A}_0, \mathbf{A}_1, \mathbf{A}_2, \mathbf{H}_0, \mathbf{H}_1, \mathbf{H}_2]$ represent all parameters of the regression coefficients and residual covariance matrices. Suppose

the yield data is balanced, N bonds for T months and $n = N \times T$ total observations. Furthermore consider K macro factors in addition to the 3 factors of dynamic Nelson-Siegel model, K can be zero for the case without macroeconomic variable. The dimension of all matrices are listed as follows $\mathbf{y}_t, \boldsymbol{\varepsilon}_t$: $N \times 1$, $\boldsymbol{\Lambda}$: $N \times 3$, $\mathbf{f}_t, \mathbf{F}_t, \boldsymbol{\mu}_0, \boldsymbol{\mu}_1, \boldsymbol{\mu}_2, \boldsymbol{\eta}_t$: $(3 + K) \times 1$, $\mathbf{A}_0, \mathbf{A}_1, \mathbf{A}_2$: $(3 + K) \times (3 + K)$, \mathbf{Q} : $N \times N$, $\mathbf{H}_0, \mathbf{H}_1, \mathbf{H}_2$: $(3 + K) \times (3 + K)$. The initial values for parameters are obtained from two step approach results. Initial values of Kalman filter \mathbf{F}_0 and \mathbf{P}_0 are equal to estimates by using Econometrics Toolbox state-space models (SSM) in MATLAB. The prior for parameters and full Gibbs sampler for posterior inference are as follows.

- Prior specification for different parameters
 - Spike-and-slab prior: $\xi_0^2 = 10^{-5}, \xi_1^2 = 1$.
 - Decay parameter λ prior: $a = 0.01, b = 0.1$.
 - Diagonal elements σ_i^2 of \mathbf{Q} prior: $\alpha = 5, \beta = 0.05$.
 - Factor mean $\boldsymbol{\mu}$ prior: $\underline{\boldsymbol{\mu}}$ is equal to initial value of $\boldsymbol{\mu}$, $\mathbf{B} = \text{diag}(10)_{3+K}$.
 - Covariance matrix \mathbf{H} prior: \mathbf{m}_0 and \mathbf{M}_0 are set according to initial value of \mathbf{H} , i.e., prior mean closing to initial values.
- $\tilde{\mathbf{F}}_T \mid \boldsymbol{\Omega}, \tilde{\mathbf{y}}_T, \boldsymbol{\Lambda}, \mathbf{Q}, \boldsymbol{\mu}_0, \boldsymbol{\mu}_1, \boldsymbol{\mu}_2$. Sampling latent factors $\tilde{\mathbf{F}}_t$ conditional on all other parameters is achieved by Kalman filter/smoother. Given $\boldsymbol{\Omega}$ and \mathbf{F}_0 , the posterior distribution of $\tilde{\mathbf{F}}_T$ can be decomposed as a set of conditionals

$$p(\tilde{\mathbf{F}}_T \mid \tilde{\mathbf{y}}_T) = p(\mathbf{F}_T \mid \tilde{\mathbf{y}}_T) \prod_{t=1}^{T-1} p(\mathbf{F}_t \mid \mathbf{F}_{t+1}, \tilde{\mathbf{y}}_t).$$

The above equation suggests that the factors $\tilde{\mathbf{F}}_T$ can be sampled sequentially by

Kalman filter, where all the conditionals are defined as

$$\begin{aligned}
\hat{\mathbf{F}}_{t|t-1} &= \mathbf{A}_{z_{t-1}} \mathbf{F}_{t-1|t-1} \\
\hat{\mathbf{P}}_{t|t-1} &= \mathbf{A}_{z_{t-1}} \mathbf{P}_{t-1|t-1} \mathbf{A}_{z_{t-1}}^T + \mathbf{H}_{z_t} \\
\mathbf{K}_t &= \hat{\mathbf{P}}_{t|t-1} \mathbf{\Lambda}^T (\mathbf{\Lambda} \hat{\mathbf{P}}_{t|t-1} \mathbf{\Lambda}^T + \mathbf{Q})^{-1} \\
\mathbf{F}_{t|t} &= \hat{\mathbf{F}}_{t|t-1} + \mathbf{K}_t (\mathbf{y}_t - \mathbf{\Lambda} \hat{\mathbf{F}}_{t|t-1} - \mathbf{\Lambda} \boldsymbol{\mu}_{z_t}) \\
\mathbf{P}_{t|t} &= (\mathbf{I} - \mathbf{K}_t \mathbf{\Lambda}) \hat{\mathbf{P}}_{t|t-1}.
\end{aligned}$$

The sampling steps are

$$- \mathbf{F}_T \mid \tilde{\mathbf{y}}_T \sim N(\mathbf{F}_{T|T}, \mathbf{P}_{T|T}), \text{ where}$$

$$\begin{aligned}
\mathbf{F}_{T|T} &= \hat{\mathbf{F}}_{T|T-1} + \mathbf{K}_T (\mathbf{y}_T - \mathbf{\Lambda} \hat{\mathbf{F}}_{T|T-1} - \mathbf{\Lambda} \boldsymbol{\mu}_{z_T}) \\
\mathbf{P}_{T|T} &= (\mathbf{I} - \mathbf{K}_T \mathbf{\Lambda}) \hat{\mathbf{P}}_{T|T-1}
\end{aligned}$$

$$- \mathbf{F}_t \mid \mathbf{F}_{t+1}, \tilde{\mathbf{y}}_t \sim N(\mathbf{F}_{t|t, \mathbf{F}_{t+1}}, \mathbf{P}_{t|t, \mathbf{F}_{t+1}}), \text{ where}$$

$$\begin{aligned}
\mathbf{F}_{t|t, \mathbf{F}_{t+1}} &= \mathbf{F}_{t|t} + \mathbf{P}_{t|t} \mathbf{A}_{z_t}^T (\mathbf{A}_{z_t} \mathbf{P}_{t|t} \mathbf{A}_{z_t}^T + \mathbf{H}_{z_{t+1}})^{-1} (\mathbf{F}_{t+1} - \mathbf{A}_{z_t} \mathbf{F}_{t|t}) \\
\mathbf{P}_{t|t, \mathbf{F}_{t+1}} &= \mathbf{P}_{t|t} - \mathbf{P}_{t|t} \mathbf{A}_{z_t}^T (\mathbf{A}_{z_t} \mathbf{P}_{t|t} \mathbf{A}_{z_t}^T + \mathbf{H}_{z_{t+1}})^{-1} \mathbf{A}_{z_t} \mathbf{P}_{t|t}
\end{aligned}$$

- $\mathbf{Q} \mid \tilde{\mathbf{F}}_T, \tilde{\mathbf{y}}_T, \boldsymbol{\Omega}, \boldsymbol{\mu}_0, \boldsymbol{\mu}_1, \boldsymbol{\mu}_2, \mathbf{\Lambda}$. Yield residual covariance matrix $\mathbf{Q} = \text{diag}(\sigma_1^2, \dots, \sigma_N^2)$ is assumed to be diagonal. The update of each σ_i^2 term follows the standard inverse-Gamma conjugate sampling. For simplicity, we show the update of one regime, and multiple regimes proceed similarly.

$$\sigma_i^2 \mid \tilde{\mathbf{F}}_T, \tilde{\mathbf{y}}_T, \boldsymbol{\Omega}, \boldsymbol{\mu}_0, \boldsymbol{\mu}_1, \boldsymbol{\mu}_2, \mathbf{\Lambda} \sim IG \left(\alpha + \frac{T}{2}, \beta + \frac{1}{2} \sum_{t=1}^T (\mathbf{y}_{ti} - \mathbf{\Lambda}_i \mathbf{F}_t - \mathbf{\Lambda}_i \boldsymbol{\mu}_{z_t})^2 \right),$$

where $\mathbf{\Lambda}_i$ is the i -th row in $\mathbf{\Lambda}$ and \mathbf{y}_{ti} is the i -th row in \mathbf{y}_t , $i = 1, 2, \dots, N$.

- $\mathbf{H}_g \mid \tilde{\mathbf{F}}_T, \mathbf{A}_0, \mathbf{A}_1, \mathbf{A}_2$. Let T_g be number of time periods in the regime g , and for t

satisfying the regime indicator $z_t = g$, $\eta_t \sim N(0, \mathbf{H}_g)$. The update step is

$$\mathbf{H}_g \mid \tilde{\mathbf{F}}_T, \mathbf{A}_0, \mathbf{A}_1, \mathbf{A}_2, \boldsymbol{\mu}_0, \boldsymbol{\mu}_1, \boldsymbol{\mu}_2 \sim IW(\mathbf{m}_0 + T_g, \mathbf{M}_0 + \mathbf{G}_g),$$

$$\text{where } \mathbf{G}_g = \sum_{t:z_t=g} (\mathbf{F}_t - \mathbf{A}_{z_{t-1}} \mathbf{F}_{t-1})(\mathbf{F}_t - \mathbf{A}_{z_{t-1}} \mathbf{F}_{t-1})^T.$$

- $\mathbf{A}_g \mid \gamma_g, \tilde{\mathbf{F}}_T, \mathbf{H}_0, \mathbf{H}_1, \mathbf{H}_2$. Let $\mathbf{a}_g = \text{vec}(\mathbf{A}_g^T)$, $\gamma_g = \text{vec}((\gamma^g)^T)$.

$$\begin{aligned} \pi(\mathbf{a}_g \mid \tilde{\mathbf{F}}_T, \mathbf{H}_0, \mathbf{H}_1, \mathbf{H}_2, \gamma_g) &\propto p(\mathbf{F}_{t+1:z_t=g} \mid \mathbf{a}_g, \mathbf{H}_0, \mathbf{H}_1, \mathbf{H}_2, \gamma_g) \pi(\mathbf{a}_g \mid \gamma_g) \\ &\propto \exp \left\{ -\frac{1}{2} \left[\mathbf{a}_g^T \left(\sum_{t:z_t=g} \mathbf{H}_{z_{t+1}}^{-1} \otimes (\mathbf{F}_t \mathbf{F}_t^T) \right) \mathbf{a}_g - 2 \mathbf{a}_g^T \left(\sum_{t:z_t=g} \text{vec}(\mathbf{F}_t \mathbf{F}_{t+1}^T \mathbf{H}_{z_{t+1}}^{-1}) \right) \right] \right\} \times \prod_{j,k=1}^3 \pi(\mathbf{a}_{jk}^g \mid \gamma_{jk}^g) \\ &\propto \exp \left\{ -\frac{1}{2} \left[\mathbf{a}_g^T \left(\sum_{t:z_t=g} \mathbf{H}_{z_{t+1}}^{-1} \otimes (\mathbf{F}_t \mathbf{F}_t^T) \right) \mathbf{a}_g - 2 \mathbf{a}_g^T \left(\sum_{t:z_t=g} \text{vec}(\mathbf{F}_t \mathbf{F}_{t+1}^T \mathbf{H}_{z_{t+1}}^{-1}) \right) \right] \right\} \times \prod_{j,k=1}^3 \exp \left\{ -\frac{1}{2 \xi_{\gamma_{jk}^g}^2} a_{jk}^g{}^2 \right\} \\ &\propto \exp \left\{ -\frac{1}{2} \left[\mathbf{a}_g^T \left(\mathbf{U}_g^{-1} + \sum_{t:z_t=g} \mathbf{H}_{z_{t+1}}^{-1} \otimes (\mathbf{F}_t \mathbf{F}_t^T) \right) \mathbf{a}_g - 2 \mathbf{a}_g^T \left(\sum_{t:z_t=g} \text{vec}(\mathbf{F}_t \mathbf{F}_{t+1}^T \mathbf{H}_{z_{t+1}}^{-1}) \right) \right] \right\}, \end{aligned}$$

where $\mathbf{U}_g = \text{diag}(\xi_{\gamma_{jk}^g}^2)$, $j, k = 1, 2, 3$. Draw \mathbf{a}_g from conditional posterior $N(\bar{\mathbf{a}}_g, \bar{\mathbf{D}}_g)$, where

$$\bar{\mathbf{D}}_g = (\mathbf{U}_g^{-1} + \sum_{t:z_t=g} \mathbf{H}_{z_{t+1}}^{-1} \otimes (\mathbf{F}_t \mathbf{F}_t^T))^{-1}, \quad \bar{\mathbf{a}}_g = \bar{\mathbf{D}}_g \left(\sum_{t:z_t=g} \text{vec}(\mathbf{F}_t \mathbf{F}_{t+1}^T \mathbf{H}_{z_{t+1}}^{-1}) \right).$$

- $\gamma_{jk}^g \mid \gamma_{-jk}^g, \tilde{\mathbf{F}}_T, \mathbf{H}_0, \mathbf{H}_1, \mathbf{H}_2$. γ_{-jk}^g represents the remaining elements except the (j, k) -th element of γ^g .

$$\begin{aligned} \pi(\gamma_g \mid \tilde{\mathbf{F}}_T, \mathbf{H}_0, \mathbf{H}_1, \mathbf{H}_2) &\propto \int p(\mathbf{F}_{t+1:z_t=g} \mid \mathbf{a}_g, \mathbf{H}_0, \mathbf{H}_1, \mathbf{H}_2, \gamma_g) p(\mathbf{a}_g \mid \gamma_g) \pi(\gamma_g) d\mathbf{a}_g \\ &\propto \int \exp \left\{ -\frac{1}{2} \left[\mathbf{a}_g^T \left(\sum_{t:z_t=g} \mathbf{H}_{z_{t+1}}^{-1} \otimes (\mathbf{F}_t \mathbf{F}_t^T) \right) \mathbf{a}_g - 2 \mathbf{a}_g^T \left(\sum_{t:z_t=g} \text{vec}(\mathbf{F}_t \mathbf{F}_{t+1}^T \mathbf{H}_{z_{t+1}}^{-1}) \right) \right] \right\} \\ &\times |\mathbf{U}_g|^{-\frac{1}{2}} \exp \left(-\frac{1}{2} \mathbf{a}_g^T \mathbf{U}_g^{-1} \mathbf{a}_g \right) w^{\sum \gamma_{jk}^g} (1-w)^{\sum (1-\gamma_{jk}^g)} d\mathbf{a}_g \\ &= |\mathbf{U}_g|^{-\frac{1}{2}} w^{\sum \gamma_{jk}^g} (1-w)^{\sum (1-\gamma_{jk}^g)} \\ &\times \int \exp \left\{ -\frac{1}{2} \left[\mathbf{a}_g^T \left(\mathbf{U}_g^{-1} + \sum_{t:z_t=g} \mathbf{H}_{z_{t+1}}^{-1} \otimes (\mathbf{F}_t \mathbf{F}_t^T) \right) \mathbf{a}_g - 2 \mathbf{a}_g^T \left(\sum_{t:z_t=g} \text{vec}(\mathbf{F}_t \mathbf{F}_{t+1}^T \mathbf{H}_{z_{t+1}}^{-1}) \right) \right] \right\} \\ &\propto |\mathbf{U}_g|^{-\frac{1}{2}} |\bar{\mathbf{D}}_g|^{\frac{1}{2}} \exp \left(\frac{1}{2} \bar{\mathbf{a}}_g^T \bar{\mathbf{D}}_g^{-1} \bar{\mathbf{a}}_g \right) w^{\sum \gamma_{jk}^g} (1-w)^{\sum (1-\gamma_{jk}^g)} \\ &= |\mathbf{U}_g|^{-\frac{1}{2}} |\bar{\mathbf{D}}_g|^{\frac{1}{2}} \exp \left(\frac{1}{2} \mathbf{l}^T \bar{\mathbf{D}}_g \mathbf{l} \right) w^{\sum \gamma_{jk}^g} (1-w)^{\sum (1-\gamma_{jk}^g)}, \end{aligned}$$

where $\mathbf{l} = \sum_{t:z_t=g} \text{vec}(\mathbf{F}_t \mathbf{F}_{t+1}^T \mathbf{H}_{z_{t+1}}^{-1})$. Therefore the conditional posterior of $\gamma_{jk}^g \mid \gamma_{-jk}^g$ is

$$\pi(\gamma_{jk}^g \mid \gamma_{-jk}^g, \tilde{\mathbf{F}}_T, \mathbf{H}_0, \mathbf{H}_1, \mathbf{H}_2) \propto \xi_{\gamma_{jk}^g}^{-1} \mid \bar{\mathbf{D}}_g \mid^{\frac{1}{2}} \exp\left(\frac{1}{2} \mathbf{l}^T \bar{\mathbf{D}}_g \mathbf{l}\right) w^{\sum \gamma_{jk}^g} (1-w)^{\sum (1-\gamma_{jk}^g)},$$

which is a Bernoulli distribution. For diagonal elements of \mathbf{A}_g , force $\gamma_{jk}^g = 1$. It's natural to assume that the dynamics of one factor is related to its historical values, so we don't impose spike-and-slab prior on diagonal elements of transition matrix \mathbf{A} and let the corresponding γ fixed at 1.

- $\boldsymbol{\mu}_g \mid \tilde{\mathbf{F}}_T, \tilde{\mathbf{y}}_T, \boldsymbol{\Lambda}, \mathbf{Q}$. Assume there are T_g time points in regime g , and in regime g , the likelihood is

$$\begin{aligned} p(\mathbf{y}_{t:z_t=g} \mid \boldsymbol{\mu}_g) &\propto \prod_{t:z_t=g} \exp\left\{-\frac{1}{2} \boldsymbol{\varepsilon}_t^T \mathbf{Q}^{-1} \boldsymbol{\varepsilon}_t\right\} \\ &\propto \exp\left\{-\frac{1}{2} \left[\boldsymbol{\mu}_g^T (T_g \boldsymbol{\Lambda}^T \mathbf{Q}^{-1} \boldsymbol{\Lambda}) \boldsymbol{\mu}_g - 2 \boldsymbol{\mu}_g^T \left(\sum_{t:z_t=g} (\boldsymbol{\Lambda}^T \mathbf{Q}^{-1} \mathbf{y}_t - \boldsymbol{\Lambda}^T \mathbf{Q}^{-1} \boldsymbol{\Lambda} \mathbf{F}_t) \right) \right] \right\}. \end{aligned}$$

The posterior distribution is

$$\boldsymbol{\mu}_g \mid \tilde{\mathbf{F}}_T, \tilde{\mathbf{y}}_T, \boldsymbol{\Lambda}, \mathbf{Q} \sim N(\bar{\boldsymbol{\mu}}_g, \bar{\mathbf{B}}_g),$$

where

$$\begin{aligned} \bar{\mathbf{B}}_g &= (\underline{\mathbf{B}}^{-1} + T_g \boldsymbol{\Lambda}^T \mathbf{Q}^{-1} \boldsymbol{\Lambda})^{-1} \\ \bar{\boldsymbol{\mu}}_g &= \bar{\mathbf{B}}_g \left(\underline{\mathbf{B}}^{-1} \underline{\boldsymbol{\mu}} + \sum_{t:z_t=g} (\boldsymbol{\Lambda}^T \mathbf{Q}^{-1} \mathbf{y}_t - \boldsymbol{\Lambda}^T \mathbf{Q}^{-1} \boldsymbol{\Lambda} \mathbf{F}_t) \right). \end{aligned}$$

- $\lambda \mid \tilde{\mathbf{F}}_T, \boldsymbol{\mu}_0, \boldsymbol{\mu}_1, \boldsymbol{\mu}_2, \tilde{\mathbf{y}}_T, \mathbf{Q}$. We use random walk Metropolis-Hastings algorithm to estimate λ . Superscript t indicates the t -th update of MCMC.
 - Generate λ^* from proposal distribution $J_t(\lambda^* \mid \lambda^{(t-1)}) = U(0.01, 0.1)$.
 - Compute acceptance ratio r . $p_0(\lambda) = p(\lambda \mid \tilde{\mathbf{F}}_T, \boldsymbol{\mu}_0, \boldsymbol{\mu}_1, \boldsymbol{\mu}_2, \tilde{\mathbf{y}}_T, \mathbf{Q})$ is the target

posterior distribution.

$$r = \frac{p_0(\lambda^*)}{p_0(\lambda^{(t-1)})} \times \frac{J_t(\lambda^{(t-1)} \mid \lambda^*)}{J_t(\lambda^* \mid \lambda^{(t-1)})} = \frac{p_0(\lambda^*)}{p_0(\lambda^{(t-1)})}$$

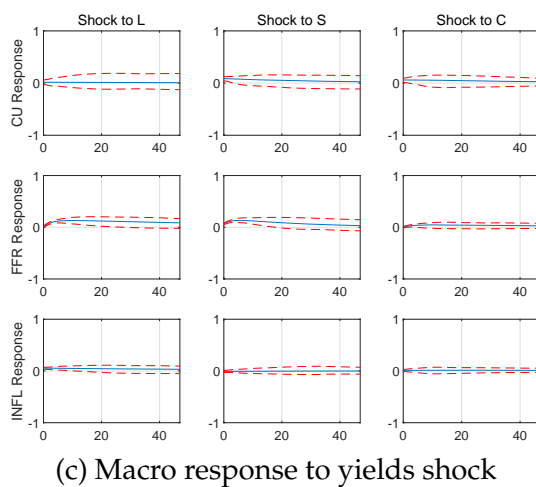
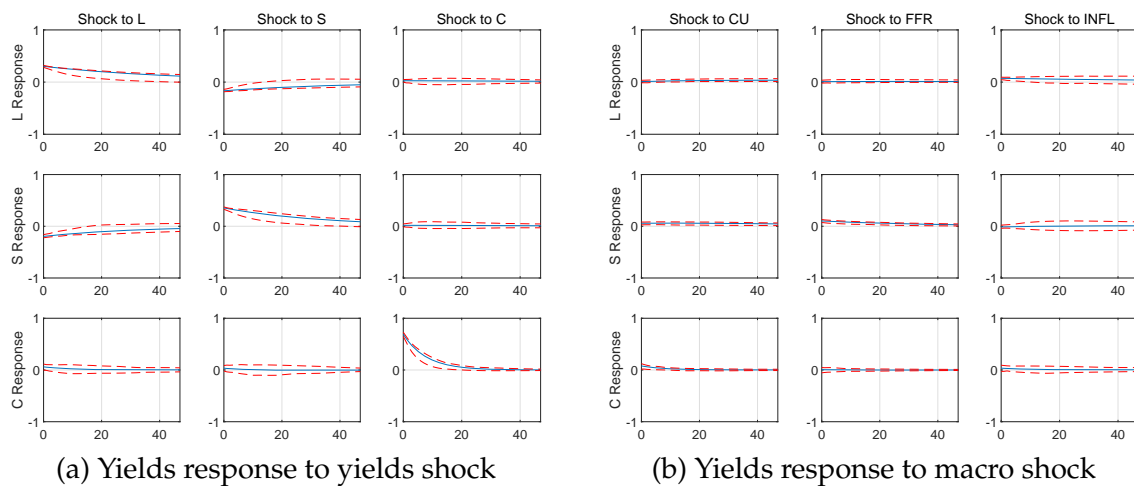
– Sample $u \sim U(0, 1)$, if $u < r$, set $\lambda^t = \lambda^*$, else set $\lambda^t = \lambda^{(t-1)}$.

The conditional posterior distribution is

$$\begin{aligned} p(\lambda \mid \tilde{\mathbf{F}}_T, \boldsymbol{\mu}_0, \boldsymbol{\mu}_1, \boldsymbol{\mu}_2, \tilde{\mathbf{y}}_T, \mathbf{Q}) &\propto p(\tilde{\mathbf{y}}_T \mid \lambda, \tilde{\mathbf{F}}_T, \boldsymbol{\mu}_0, \boldsymbol{\mu}_1, \boldsymbol{\mu}_2, \mathbf{Q}) \times p(\lambda). \\ &= \prod_{t=1}^T p(\mathbf{y}_t \mid \boldsymbol{\mu}_0, \boldsymbol{\mu}_1, \boldsymbol{\mu}_2, \lambda) p(\lambda) \\ &\propto \prod_{t=1}^T \frac{1}{\sqrt{2\pi}} \mid \mathbf{Q} \mid^{-\frac{1}{2}} \exp \left\{ -\frac{1}{2} (\mathbf{y}_t - \boldsymbol{\Lambda}(\mathbf{F}_t + \boldsymbol{\mu}_{z_t}))^T \mathbf{Q}^{-1} (\mathbf{y}_t - \boldsymbol{\Lambda}(\mathbf{F}_t + \boldsymbol{\mu}_{z_t})) \right\} \\ &\propto \exp \left\{ -\frac{1}{2} \sum_{t=1}^T (\mathbf{y}_t - \boldsymbol{\Lambda}(\mathbf{F}_t + \boldsymbol{\mu}_{z_t}))^T \mathbf{Q}^{-1} (\mathbf{y}_t - \boldsymbol{\Lambda}(\mathbf{F}_t + \boldsymbol{\mu}_{z_t})) \right\}. \end{aligned}$$

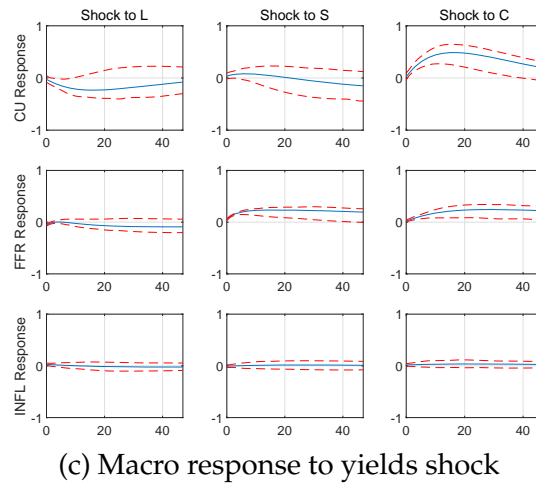
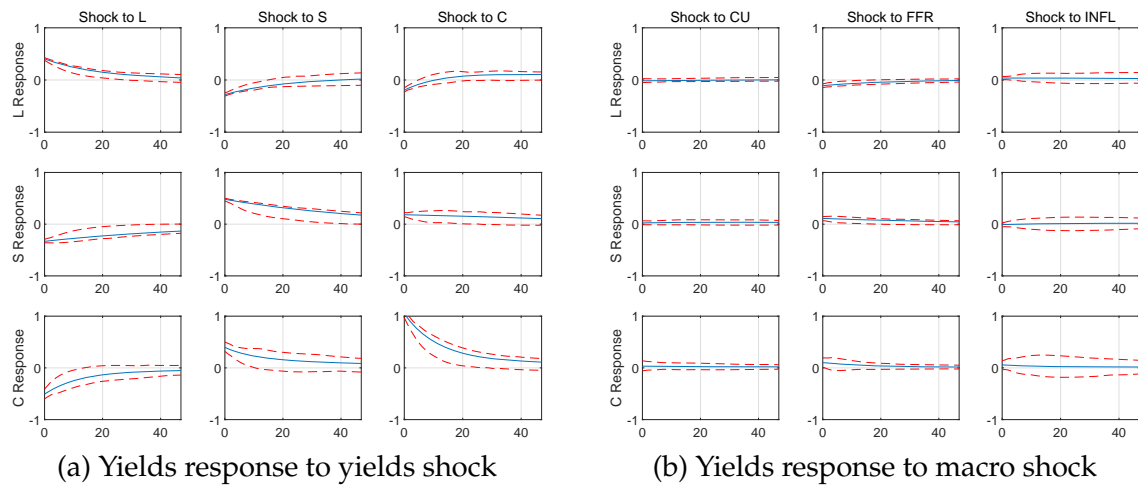
B Additional Results for Impulse Responses

Figure B1: Impulse Responses of Regime 2, Three-Regime Yields-Macro Model



Notes: This plot summarizes impulse responses for Regime 2. Blue line indicates dynamic response and the two red dashed lines are upper and lower bound of credible bands.

Figure B2: Impulse Responses of Regime 3, Three-Regime Yields-Macro Model



Notes: This plot summarizes impulse responses for Regime 3. Blue line indicates dynamic response and the two red dashed lines are upper and lower bound of credible bands.

References

- Ang, A. and G. Bekaert (2002). Regime switches in interest rates. *Journal of Business & Economic Statistics* 20(2), 163–182.
- Ang, A. and M. Piazzesi (2003). A no-arbitrage vector autoregression of term structure dynamics with macroeconomic and latent variables. *Journal of Monetary Economics* 50(4), 745–787.
- Bansal, R. and H. Zhou (2002). Term structure of interest rates with regime shifts. *Journal of Finance* 57(5), 1997–2043.
- Bauer, M. D. and G. D. Rudebusch (2017). Resolving the spanning puzzle in macro-finance term structure models. *Review of Finance* 21(2), 511–553.
- Bekaert, G., E. Engstrom, and A. Ermolov (2021). Macro risks and the term structure of interest rates. *Journal of Financial Economics* 141(2), 479–504.
- Breiman, L., J. H. Friedman, R. A. Olshen, and C. J. Stone (1984). *Classification And Regression Trees*, CRC Press.
- Chernov, M. and P. Mueller (2012). The term structure of inflation expectations. *Journal of Financial Economics* 106(2), 367–394.
- Chipman, H. A., E. I. George, and R. E. McCulloch (2010). BART: Bayesian additive regression trees. *Annals of Applied Statistics* 4(1), 266–298.
- Cong, L. W., G. Feng, J. He, and X. He (2022). Growing the efficient frontier on panel trees. Technical Report w30805.
- Cong, L. W., G. Feng, J. He, and J. Li (2023). Sparse modeling under grouped heterogeneity with an application to asset pricing. Technical report, National Bureau of Economic Research.
- Coroneo, L., D. Giannone, and M. Modugno (2016). Unspanned macroeconomic factors in the yield curve. *Journal of Business & Economic Statistics* 34(3), 472–485.
- Dai, Q., K. J. Singleton, and W. Yang (2007). Regime shifts in a dynamic term structure model of U.S. treasury bond yields. *Review of Financial Studies* 20(5), 1669–1706.
- Dewachter, H. and M. Lyrio (2006). Macro factors and the term structure of interest rates. *Journal of Money, Credit and Banking* 38(1), 119–140.
- Diebold, F. X. and C. Li (2006). Forecasting the term structure of government bond yields. *Journal of Econometrics* 130(2), 337–364.

- Diebold, F. X. and G. D. Rudebusch (2013). *Yield Curve Modeling and Forecasting: The Dynamic Nelson-Siegel Approach*, Princeton University Press.
- Diebold, F. X., G. D. Rudebusch, and S. B. Aruoba (2006). The macroeconomy and the yield curve: a dynamic latent factor approach. *Journal of Econometrics* 131(1-2), 309–338.
- Duffee, G. R. (2011). Information in (and not in) the term structure. *Review of Financial Studies* 24(9), 2895–2934.
- Feng, G., J. He, J. Li, L. Sarno, and Q. Zhang (2024). Currency return dynamics: what is the role of U.S. macroeconomic regimes? Technical report, City University of Hong Kong.
- George, E. I. and R. E. McCulloch (1993). Variable selection via Gibbs sampling. *Journal of the American Statistical Association* 88(423), 881–889.
- Gray, S. F. (1996). Modeling the conditional distribution of interest rates as a regime-switching process. *Journal of Financial Economics* 42(1), 27–62.
- Hamilton, J. D. (1989). A new approach to the economic analysis of nonstationary time series and the business cycle. *Econometrica* 57(2), 357–384.
- He, J. and P. R. Hahn (2023). Stochastic tree ensembles for regularized nonlinear regression. *Journal of the American Statistical Association* 118(541), 551–570.
- He, J., S. Yalov, and P. R. Hahn (2019). XBART: Accelerated Bayesian additive regression trees. In *The 22nd International Conference on Artificial Intelligence and Statistics*, pp. 1130–1138. PMLR.
- Hevia, C., M. Gonzalez-Rozada, M. Sola, and F. Spagnolo (2015). Estimating and forecasting the yield curve using a Markov switching dynamic Nelson and Siegel model. *Journal of Applied Econometrics* 30(6), 987–1009.
- Joslin, S., M. Pribsch, and K. J. Singleton (2014). Risk premiums in dynamic term structure models with unspanned macro risks. *Journal of Finance* 69(3), 1197–1233.
- Kim, C.-J. (1994). Dynamic linear models with Markov-switching. *Journal of Econometrics* 60(1), 1–22.
- Koop, G., M. Pesaran, and S. Potter (1996). Impulse response analysis in nonlinear multivariate models. *Journal of Econometrics* 74(1), 119–147.
- Krantsevich, N., J. He, and P. R. Hahn (2023). Stochastic tree ensembles for estimating heterogeneous effects. In *International Conference on Artificial Intelligence and Statistics*, pp. 6120–6131. PMLR.

- Liu, Y. and J. C. Wu (2021). Reconstructing the yield curve. *Journal of Financial Economics* 142(3), 1395–1425.
- Ludvigson, S. C. and S. Ng (2009). Macro factors in bond risk premia. *Review of Financial Studies* 22(12), 5027–5067.
- Nelson, C. R. and A. F. Siegel (1987). Parsimonious modeling of yield curves. *Journal of Business* 60(4), 473–489.
- Patton, A. J. and Y. Simsek (2023). Generalized autoregressive score trees and forests. *arXiv:2305.18991*.
- Sims, C. (1980). Macroeconomics and reality. *Econometrica* 48, 1–48.
- Xiang, J. and X. Zhu (2013). A regime-switching Nelson–Siegel term structure model and interest rate forecasts. *Journal of Financial Econometrics* 11(3), 522–555.